

Aurora Isoform Selectivity: Design and Synthesis of Imidazo[4,5-*b*]pyridine Derivatives as Highly Selective Inhibitors of Aurora-A Kinase in Cells

Vassilios Bayetsias,^{*,†} Amir Faisal,[†] Simon Crumpler,[†] Nathan Brown,[†] Magda Kosmopoulou,[‡] Amar Joshi,[§] Butrus Atrash,[†] Yolanda Pérez-Fuertes,[†] Jessica A. Schmitt,[†] Katherine J. Boxall,[†] Rosemary Burke,[†] Chongbo Sun,[†] Sian Avery,[†] Katherine Bush,[†] Alan Henley,[†] Florence I. Raynaud,[†] Paul Workman,[†] Richard Bayliss,^{‡,§} Spiros Linardopoulos,^{†,||} and Julian Blagg^{*,†}

[†]Cancer Research UK Cancer Therapeutics Unit, Division of Cancer Therapeutics, The Institute of Cancer Research, London SM2 5NG, United Kingdom

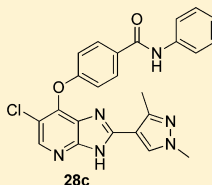
[‡]Division of Structural Biology, The Institute of Cancer Research, Chester Beatty Laboratories, London SW3 6JB, United Kingdom

[§]Department of Biochemistry, University of Leicester, Lancaster Road, Leicester LE1 9HN, United Kingdom

^{||}The Breakthrough Breast Cancer Research Centre, Division of Breast Cancer Research, The Institute of Cancer Research, London SW3 6JB, United Kingdom

S Supporting Information

ABSTRACT: Aurora-A differs from Aurora-B/C at three positions in the ATP-binding pocket (L215, T217, and R220). Exploiting these differences, crystal structures of ligand–Aurora protein interactions formed the basis of a design principle for imidazo[4,5-*b*]pyridine-derived Aurora-A-selective inhibitors. Guided by a computational modeling approach, appropriate C7-imidazo[4,5-*b*]pyridine derivatization led to the discovery of highly selective inhibitors, such as compound **28c**, of Aurora-A over Aurora-B. In HCT116 human colon carcinoma cells, **28c** and **40f** inhibited the Aurora-A L215R and R220K mutants with IC₅₀ values similar to those seen for the Aurora-A wild type. However, the Aurora-A T217E mutant was significantly less sensitive to inhibition by **28c** and **40f** compared to the Aurora-A wild type, suggesting that the T217 residue plays a critical role in governing the observed isoform selectivity for Aurora-A inhibition. These compounds are useful small-molecule chemical tools to further explore the function of Aurora-A in cells.



Aurora-A IC₅₀ = 0.067 μM
Aurora-B IC₅₀ = 12.71 μM
In HCT116 human colon carcinoma cells:
P-T288 IC₅₀ = 0.065 μM (Aurora-A inhibition)
p-HH3 IC₅₀ = 24.65 μM (biomarker for Aurora-B inhibition)

INTRODUCTION

Over the past decade there has been extensive interest in Aurora kinases as anticancer targets.^{1–3} Aurora proteins, a family of three kinases designated as Aurora-A, -B, and -C, play key and distinct roles in different stages of mitosis^{4–8} and are overexpressed in a wide range of human malignancies.^{9–15}

Research toward the discovery of Aurora kinase modulators as cancer therapeutics led to the identification of a significant number of small-molecule inhibitors of Aurora kinases, the majority of which inhibit all three isoforms A, B, and C.¹ Compounds displaying isoform selectivity have also been reported, including AZD1152,¹⁶ a selective Aurora-B inhibitor, and **1**,¹⁷ **2**,¹⁸ **3**,¹⁹ **4**,²⁰ and **5**,²¹ which selectively inhibit Aurora-A (Figure 1). Many inhibitors of Aurora kinases have reached clinical evaluation.^{1–3} In relation to isoform selectivity, the ideal inhibitor profile (i.e., selective isoform inhibition versus pan-Aurora inhibition) is still unclear, but the ongoing clinical evaluation of Aurora inhibitors may provide new insights to better answer this question. However, it should be noted that the Aurora kinases have distinct cellular functions and their inhibition has divergent effects on cells undergoing mitosis.²²

Aurora-A is involved in the initiation of mitosis by promoting centrosome maturation and bipolar mitotic spindle formation, and its inhibition leads to increased G2/M accumulation and spindle defects.^{17,22,23} Aurora-B is part of the chromosomal passenger complex (CPC), which also includes borealin, survivin, and the inner centromere protein (INCENP), and plays a critical role in the regulation of chromosome alignment and also in cytokinesis.²³ Inhibition of Aurora-B leads to abrogation of the spindle assembly checkpoint, so that cells rapidly undergo chromosome segregation even in the presence of spindle defects.²² The effects of Aurora-B inhibition mask the effects of Aurora-A inhibition, and therefore, selective inhibitors of both Aurora-A and Aurora-B are needed to carry out detailed cell-based and in vivo studies on this kinase family.²² The role of Aurora-C during mitosis is not well understood; however, it is established that Aurora-C plays a specific role in spermatogenesis.²⁴

Received: July 23, 2013

Published: November 6, 2013

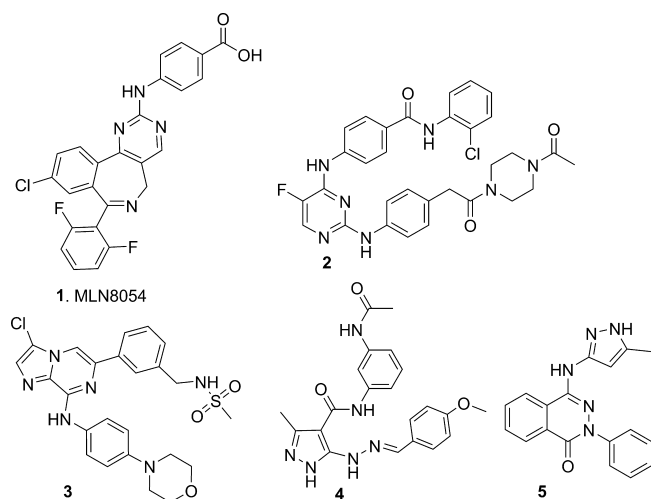


Figure 1. Selective inhibitors of Aurora-A kinase.

Other key differences between the Aurora kinases are emerging. Aurora-A alone forms a complex with N-Myc, an oncoprotein that induces neuroblastoma, which protects N-Myc from proteosomal degradation,^{25,26} and Aurora-A-selective inhibitors MLN8054 and MLN8237 disrupt the Aurora-A/N-Myc complex.²⁶ Significantly, the Aurora-A/N-Myc complex was not disrupted by the Aurora-A-selective inhibitor MK-5108, which belongs to a different chemotype.²⁶ This demonstrates the importance of having access to a range of structurally diverse selective Aurora isoform inhibitors, in addition to the existing pan-Aurora modulators. They can serve as useful small-molecule chemical tools to further explore the cellular function of Aurora proteins toward their eventual therapeutic application in cancer treatment.

We have previously reported the discovery of novel imidazo[4,5-*b*]pyridine derivatives as potent, orally bioavailable inhibitors of Aurora kinases (Figure 2),^{27,28} with a compound

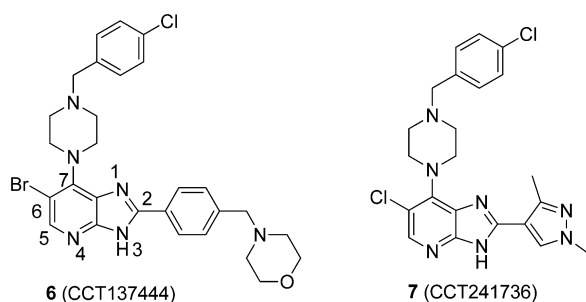


Figure 2. Imidazo[4,5-*b*]pyridine-based inhibitors of Aurora kinases.^{27,28}

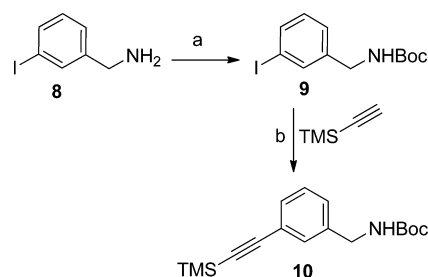
in this series being identified as a dual Aurora/FLT3 preclinical development candidate.²⁸ In parallel to this work, we also investigated the design and synthesis of Aurora-A-selective inhibitors based on the imidazo[4,5-*b*]pyridine scaffold. Herein, we report our medicinal chemistry program aimed at the identification of imidazo[4,5-*b*]pyridine- and 7-azaindole-based inhibitors displaying a high degree of selectivity for Aurora-A over Aurora-B.

CHEMISTRY

The synthesis of 7-azaindoles **16a–d** is shown in Schemes 2 and 3, with the key step being formation of the azaindole ring via a Pd-catalyzed heteroannulation reaction.^{29–31}

Starting from **8**, access was readily gained to the alkyne **10** using standard Boc protection followed by a Sonogashira cross-coupling reaction (Scheme 1). 5-Chloro-3-iodo-2-aminopyr-

Scheme 1^a



^aReagents and conditions: (a) THF, ^tBuOH, Boc₂O, room temperature, 1 h; (b) PdCl₂(PPh₃)₂, CuI, THF, Et₃N, 100 °C, microwave irradiation, 20 min.

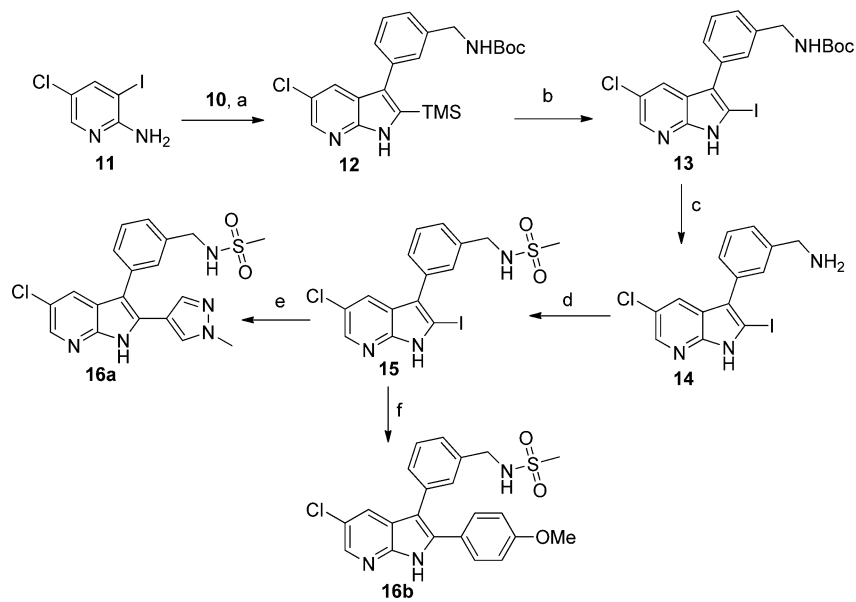
idine (**11**; Scheme 2) was obtained from 2-amino-5-chloropyridine upon treatment with *N*-iodosuccinimide and *p*-toluenesulfonic acid. Azaindole ring formation (compound **12**) was effected by reacting **11** with alkyne **10** in the presence of DABCO and Pd(PPh₃)₂Cl₂ (Scheme 2).^{29–31} The silyl/iodo exchange proceeded in good yield using *N*-iodosuccinimide as previously described.^{31,32} Subsequent Boc group removal followed by sulfonamide formation afforded the key intermediate **15**. The final products **16a,b** were then obtained via a Suzuki cross-coupling reaction (Scheme 2).

Starting from key intermediate **14**, access to the acetamide derivatives **16c,d** (Scheme 3, Table 1) was accomplished by acetylation of the amino functionality in **14** followed by the introduction of 1-methylpyrazol-4-yl and 4-methoxyphenyl via a Suzuki cross-coupling reaction (Scheme 3).

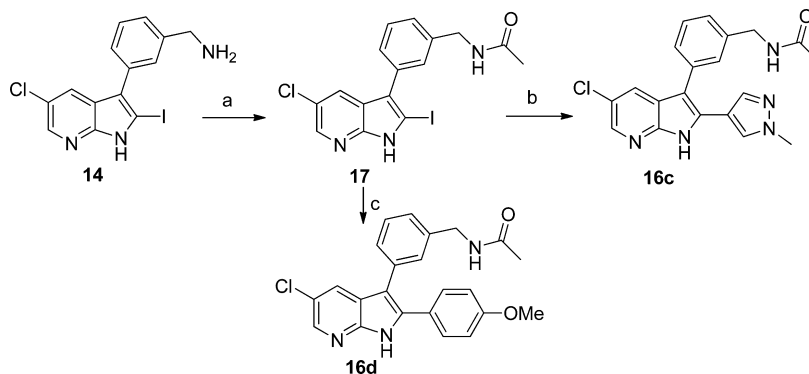
The imidazo[4,5-*b*]pyridine derivatives **21a–f**, **28a–c**, and **40a–f** (Tables 2, 3, and 34) (Table 4) were prepared by reacting 1,3-dimethyl-1*H*-pyrazole-4-carbaldehyde with the requisite 2-amino-3-nitropyridine precursor in the presence of Na₂S₂O₄ as reported previously (Schemes 4–9).^{28,33}

The key 2-amino-3-nitropyridine intermediates **20a,c,d,f** were obtained by nucleophilic displacement of the C4-chloride of 4,5-dichloro-3-nitropyridin-2-amine (**18**) with the appropriately substituted pyrrolidine (Schemes 4 and 5) or piperazine (Scheme 6) in the presence of diisopropylethylamine in 2-propanol. Intermediates **20b** and **20e** were obtained by procedures analogous to those described for their enantiomeric forms **20a** and **20d**, respectively. Starting from 4,5-dichloro-3-nitropyridin-2-amine (**18**), the benzylamino derivative **27** and *N*-phenylbenzamide derivative **29** were readily prepared by a nucleophilic substitution reaction, though for the synthesis of **29** the temperature had to be raised to 90 °C to ensure efficient displacement by the poorly nucleophilic aniline (Scheme 7).

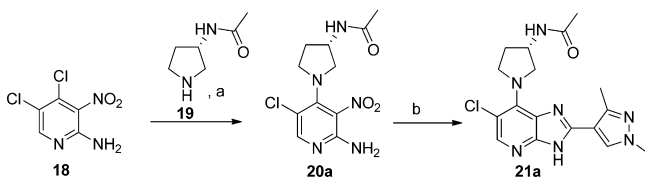
Access to the 2-amino-3-nitropyridine derivative **31** was achieved upon treatment of 4-hydroxy-*N*-phenylbenzamide (**30**), prepared as previously described,³⁴ with KO^tBu in DMF followed by the addition of 4,5-dichloro-3-nitropyridin-2-amine (Scheme 8). The C2-unsubstituted analogue of **28c**, compound **35**, was prepared from **31** by first reducing the nitro group with

Scheme 2^a

^aReagents and conditions: (a) DABCO, Pd(PPh₃)₂Cl₂, DMF, 100 °C, 92 h; (b) *N*-iodosuccinimide, DCE, 80 °C, microwave irradiation, 30 min; (c) TFA, CH₂Cl₂, room temperature, 2.5 h; (d) methanesulfonyl chloride, Et₃N, DMF, 0 °C, 4.5 h; (e) 1-methyl-4-(4,4,5,5-tetramethyl-1,3,2-dioxaborolan-2-yl)-1*H*-pyrazole, toluene, EtOH, PdCl₂(dppf), 2 M aq Na₂CO₃, 80 °C, 18 h; (f) 4-methoxyphenylboronic acid, toluene, EtOH, PdCl₂(dppf), 2 M aq Na₂CO₃, 80 °C, 16 h.

Scheme 3^a

^aReagents and conditions: (a) CH₂Cl₂, acetyl chloride, ^tPr₂NEt, -10 °C, 4 h; (b) 1-methyl-1*H*-pyrazole-4-boronic acid pinacol ester, toluene, EtOH, PdCl₂(dppf), 2 M aq Na₂CO₃, 80 °C, 16 h; (c) 4-methoxyphenylboronic acid, toluene, EtOH, PdCl₂(dppf), 2 M aq Na₂CO₃, 80 °C, 16 h.

Scheme 4^a

^aReagents and conditions: (a) 2-propanol, ^tPr₂NEt, 45 °C, 18 h; (b) 1,3-dimethyl-1*H*-pyrazole-4-carbaldehyde, EtOH, 1 M aq Na₂S₂O₄, 80 °C, 20 h.

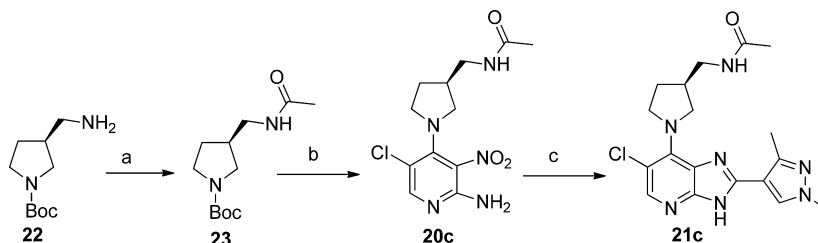
Na₂S₂O₄ and subsequently condensing the resulting diamine product **33** with trimethyl orthoformate under acidic conditions (Scheme 8). For the synthesis of the deschloro analogue of **28c** (compound **34**), the 2-amino-3-nitropyridine derivative **32**, obtained from **30** and 4-chloro-3-nitropyridin-2-amine²⁸ via an S_NAr substitution reaction, was condensed with 1,3-dimethyl-

1*H*-pyrazole-4-carbaldehyde in a manner similar to that described for **28c** (Scheme 8).

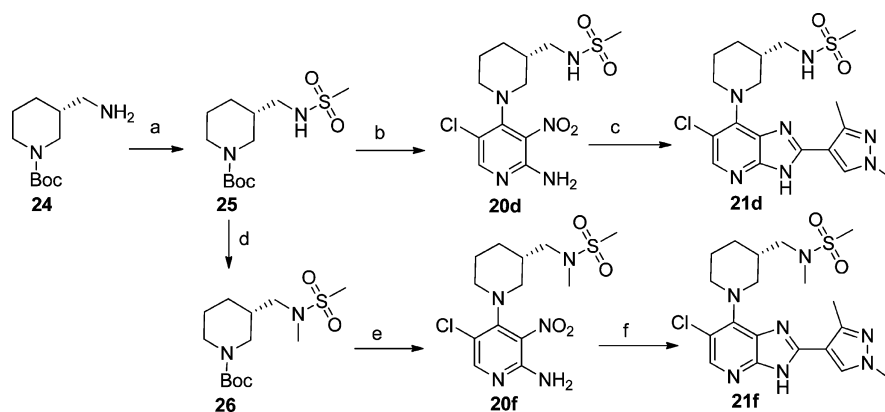
The 2-amino-3-nitro-4-phenoxy-pyridine derivatives **39a–f**, precursors to **40a–f** (Scheme 9, Table 5), were accessed by reacting 4,5-dichloro-3-nitropyridin-2-amine (**18**) with the requisite 4-hydroxybenzamide using potassium *tert*-butoxide as the base in DMF (Scheme 9). 4-Hydroxybenzamide derivatives **38a,b** and **38d–f** were all prepared from 4-acetoxybenzoic acid (**36**)³⁴ in a two-step sequence (Scheme 9); 4-hydroxy-*N*-(pyridin-3-yl)benzamide (**38c**) was commercially available. Amide bond formation was effected via acid chloride carboxyl activation, and ester hydrolysis was accomplished under alkaline conditions (Scheme 9).

RESULTS AND DISCUSSION

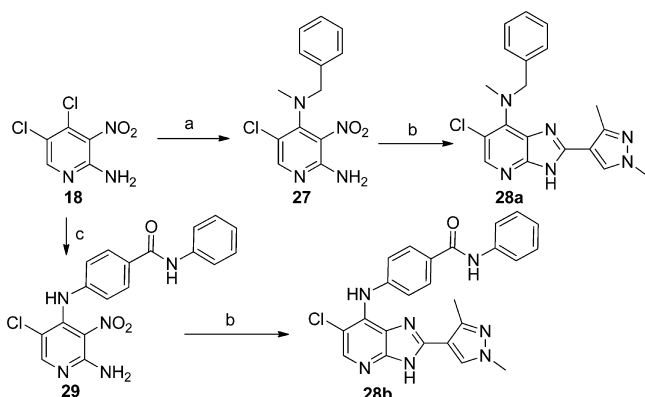
Aurora-A, -B, and -C kinases share a high degree of primary sequence homology; there are only three sequence differences in the ATP-binding site.³⁵ In Aurora-A, these residues are Leu215

Scheme 5^a

^aReagents and conditions: (a) acetic anhydride, ^tPr₂NEt, CH₂Cl₂, 0 °C to room temperature, 4 h; (b) (i) TFA, CH₂Cl₂, room temperature, 1.5 h; (ii) 4,5-dichloro-3-nitropyridin-2-amine, 2-propanol, ^tPr₂NEt, 45 °C, 20 h; (c) EtOH, 1,3-dimethyl-1H-pyrazole-4-carbaldehyde, 1 M aq Na₂S₂O₄, 80 °C, 20 h.

Scheme 6^a

^aReagents and conditions: (a) methanesulfonyl chloride, pyridine, CH₂Cl₂, room temperature, 5.5 h; (b) (i) TFA, CH₂Cl₂, room temperature, 1.5 h; (ii) 4,5-dichloro-3-nitropyridin-2-amine, 2-propanol, ^tPr₂NEt, 45 °C, 20 h; (c) EtOH, 1,3-dimethyl-1H-pyrazole-4-carbaldehyde, 1 M aq Na₂S₂O₄, 80 °C, 18 h; (d) DMF, NaH, MeI, room temperature, 1 h; (e) (i) TFA, CH₂Cl₂, room temperature, 1.5 h; (ii) 4,5-dichloro-3-nitropyridin-2-amine, 2-propanol, ^tPr₂NEt, 45 °C, 20 h; (f) EtOH, 1,3-dimethyl-1H-pyrazole-4-carbaldehyde, 1 M aq Na₂S₂O₄, 80 °C, 18 h.

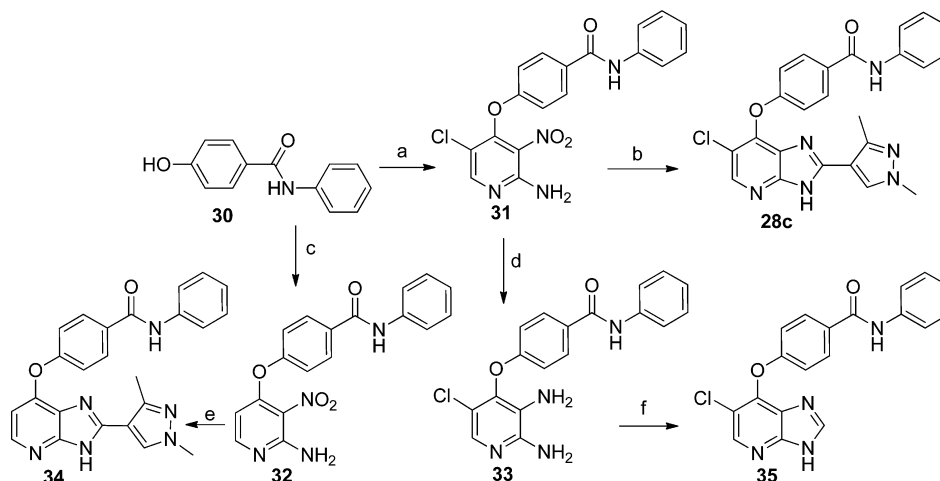
Scheme 7^a

^aReagents and conditions: (a) *N*-benzylmethylamine, 2-propanol, ^tPr₂NEt, 60 °C, 18 h; (b) 1,3-dimethyl-1H-pyrazole-4-carbaldehyde, EtOH, 1 M aq Na₂S₂O₄, 80 °C; (c) 4-amino-*N*-phenylbenzamide, 2-propanol, ^tPr₂NEt, 45 °C, 18 h, then at 90 °C for 7 h.

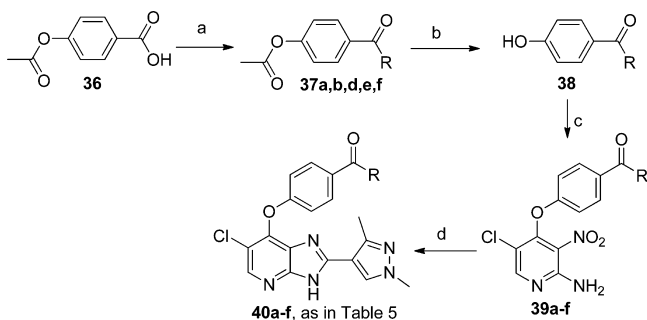
(Arg in Aurora-B/C) and Thr217 (Glu in Aurora-B/C) on the C-lobe extension of the hinge region and Arg220 (Lys in Aurora-B/C) on the α D helix. The majority of reported Aurora-A-selective inhibitors exploit the Thr217 ATP-binding site sequence difference to drive selectivity for Aurora-A inhibition over Aurora-B inhibition.^{18–20,36} Crystallographic analysis of Aurora-A in complex with small-molecule ligands provides insight into the attractiveness of targeting the Thr217 residue to

elicit Aurora isoform selectivity. For example, in the case of the imidazo[1,2-*a*]pyrazine derivative **3** (Figure 1), it was proposed that the observed selectivity for Aurora-A inhibition is driven by the interaction of a sulfonamide with the side chain of Thr217 in Aurora-A and a steric clash with the equivalent Glu residue in Aurora-B/C.¹⁹ In the crystal structure of **3** bound to Aurora-A, the Leu215 side chain points away from the active site, whereas the Arg220 is highly mobile and disordered.¹⁹ Exploitation of these two residues (i.e., Leu215 and Arg220) to drive selectivity for Aurora-A inhibition over Aurora-B/C inhibition is therefore considered to be challenging. We have previously reported the discovery of imidazo[4,5-*b*]pyridine derivatives as inhibitors of Aurora kinases, and compounds in this series were cocrystallized with Aurora-A, providing us with a clear insight into the interactions of this class of compounds with Aurora kinases.^{27,28}

The structural knowledge on the ligand–protein interactions across the imidazo[1,2-*a*]pyrazine¹⁹ and imidazo[4,5-*b*]pyridine^{27,28} series formed the basis of a design principle for imidazo[4,5-*b*]pyridine-derived Aurora-A-selective inhibition. Overlay of the imidazo[4,5-*b*]pyridine-based inhibitor **6**²⁷ with the selective inhibitor **3**¹⁹ bound to Aurora-A (Figure 3) indicated that Thr217 could be accessed via an appropriate C7-imidazo[4,5-*b*]pyridine derivatization (e.g., compounds **21c** in Scheme 5 and **21d,f** in Scheme 6) or elaboration through the N1-position of the imidazopyridine ring (e.g., 7-azaindole structures **16a–d** in Schemes 2 and 3). With regard to the former approach, we recognized that Thr217 targeting for Aurora-A-selective inhibition via C7-imidazo[4,5-*b*]pyridine

Scheme 8^a

^aReagents and conditions: (a) (i) DMF, KO^tBu, room temperature; (ii) 4,5-dichloro-3-nitropyridin-2-amine, room temperature; (b) 1,3-dimethyl-1H-pyrazole-4-carbaldehyde, DMF, 1 M aq Na₂S₂O₄, 84 °C, 20 h; (c) (i) DMF, KO^tBu, room temperature, 20 min; (ii) 4-chloro-3-nitropyridin-2-amine, 80 °C, 24 h; (d) DMSO/H₂O, Na₂S₂O₄, 80 °C, 2 h; (e) 1,3-dimethyl-1H-pyrazole-4-carbaldehyde, DMSO/H₂O, Na₂S₂O₄, 130 °C, 18 h; (f) trimethyl orthoformate, concd HCl, room temperature, 24 h.

Scheme 9^a

^aReagents and conditions: (a) (i) oxalyl chloride, CH₂Cl₂, DMF, room temperature; (ii) amine/aniline, CH₂Cl₂, room temperature; (b) MeOH or THF/H₂O, aq NaOH, room temperature; (c) (i) DMF, KO^tBu, room temperature; (ii) 4,5-dichloro-3-nitropyridin-2-amine, room temperature or heating; (d) 1,3-dimethyl-1H-pyrazole-4-carbaldehyde, DMF or DMSO, aq Na₂S₂O₄, heating.

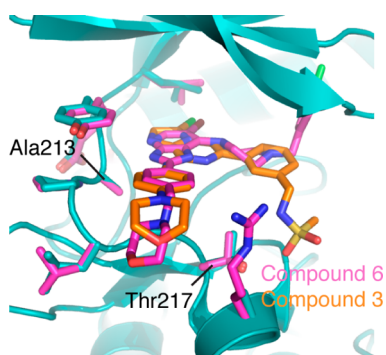


Figure 3. Overlay of 6 (PDB code 2X6D)²⁷ with 3 (PDB code 2XNG)¹⁹ bound to the ATP-binding site of Aurora-A. The hinge-binding residue Ala213 and the Thr217 residue are highlighted.

derivatization could be a challenging task due to the conformational flexibility of the proposed C7-pyrrolidine- and -piperidine-based substituents. For the latter approach, docking of C3-*N*-benzylmethanesulfonamide-derivatized 7-azaindoles into the

active site of Aurora-A indicated a mode of binding to the hinge region similar to that observed for the imidazo[4,5-*b*]pyridine-based inhibitors of Aurora^{27,28} and an interaction of the sulfonamide with Thr217.

It was also envisaged that the introduction of a 4-amino-*N*-phenylbenzamide or 4-hydroxy-*N*-phenylbenzamide substituent at the 7-position of the imidazo[4,5-*b*]pyridine ring could be beneficial for Aurora-A isoform selectivity. A 4-amino-*N*-phenylbenzamide fragment is present in 2-anilinopyrimidine-based Aurora-A-selective inhibitors reported by Aliagas-Martin et al. (see compound 2 in Figure 1).¹⁸ Docking of structure 28c (Scheme 8) into the active site of Aurora-A (PDB code 3H0Z)¹⁸ and a comparison with 2 bound to Aurora-A indicated a good overlay of the *N*-phenylbenzamide fragments (Figure 4).

Our initial efforts focused on the evaluation of the 7-azaindole scaffold (Table 1) in relation to Aurora inhibitory potency and Aurora-A isoform selectivity. Assuming a mode of binding to the hinge region similar to that observed for the imidazo[4,5-*b*]pyridine-based inhibitors,^{27,28} *p*-methoxyphenyl and 1-methylpyrazol-4-yl were chosen as optimal representative R² substituents for the 7-azaindole scaffold.^{27,28} 1-Methylpyrazol-4-yl derivatives 16a and 16c displayed higher Aurora-A and -B inhibitory potencies compared with their *p*-methoxyphenyl counterparts 16b and 16d (Table 1). On the other hand, both the sulfonamide and the acetamide groups appear to have similar Aurora-A inhibitory effects (16a vs 16c and 16b vs 16d, Table 1). Regarding selectivity for Aurora-A inhibition, although a trend to more potent Aurora-A inhibition was seen with all compounds listed in Table 1, the level of the observed isoform selectivity was not considered significant.

Attempts to cocrystallize compounds of this 7-azaindole class with Aurora-A failed to provide quality crystals; as a result we were unable to rationalize these results on a structural basis. At this point, we revisited the docking of 16a,b into the active site of Aurora-A, which indicated an additional binding mode to that previously observed. The preferred binding mode for 16a was similar to that observed with the imidazo[4,5-*b*]pyridine-based inhibitors of Aurora with the 2-aryl/heteroaryl substituent, in both imidazo[4,5-*b*]pyridine and 7-azaindole scaffolds, pointing to the solvent-accessible area^{27,28} (see Figure 5A and compound

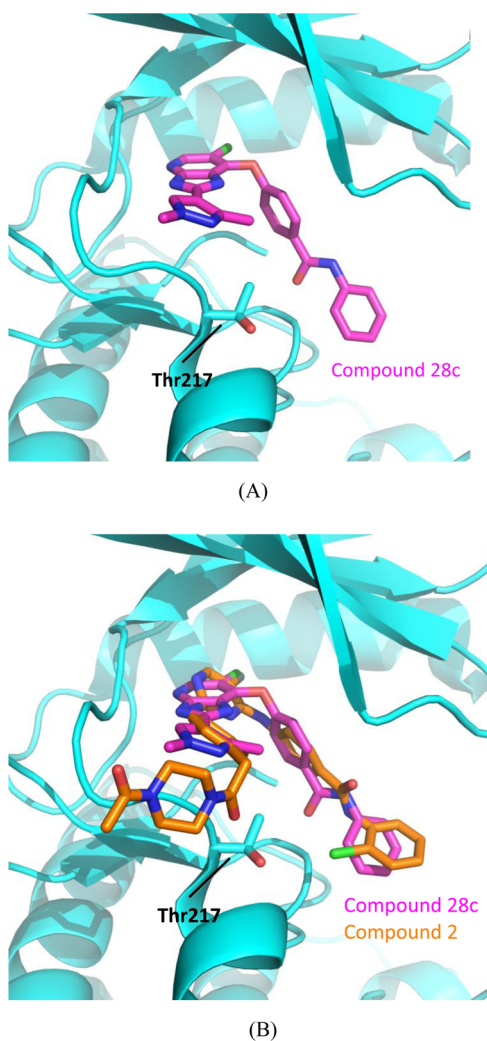
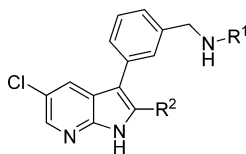


Figure 4. (A) Docking of **28c** into the active site of Aurora-A (PDB code 3H0Z)¹⁸ and (B) overlay of **28c** with the Aurora-A-selective inhibitor **2**.¹⁸

Table 1. 7-Azindole Derivatives^a



| compound | R ¹ | R ² | Aurora-A IC ₅₀ , μM | Aurora-B IC ₅₀ , μM |
|------------|----------------|----------------|-----------------------------------|-----------------------------------|
| 16a | | | 0.211 ± 0.042 | 0.441 ± 0.089 |
| 16b | | | 1.941 ± 1.160 | 7.095 ± 1.719 |
| 16c | | | 0.118 ± 0.017 | 0.097 ± 0.016 |
| 16d | | | 0.743 ± 0.392 | 1.087 ± 0.010 |

^aThe results are mean values of two independent determinations (±SD).

6 in Figure 3). However, an additional flipped binding mode was observed in docking experiments with compound **16b** compared to **16a** (compare Figure 5B with Figure 5A). It should also be noted that the *p*-methoxyphenyl derivatives **16b** and **16d** exhibited low Aurora-A inhibitory potencies. Taking all these

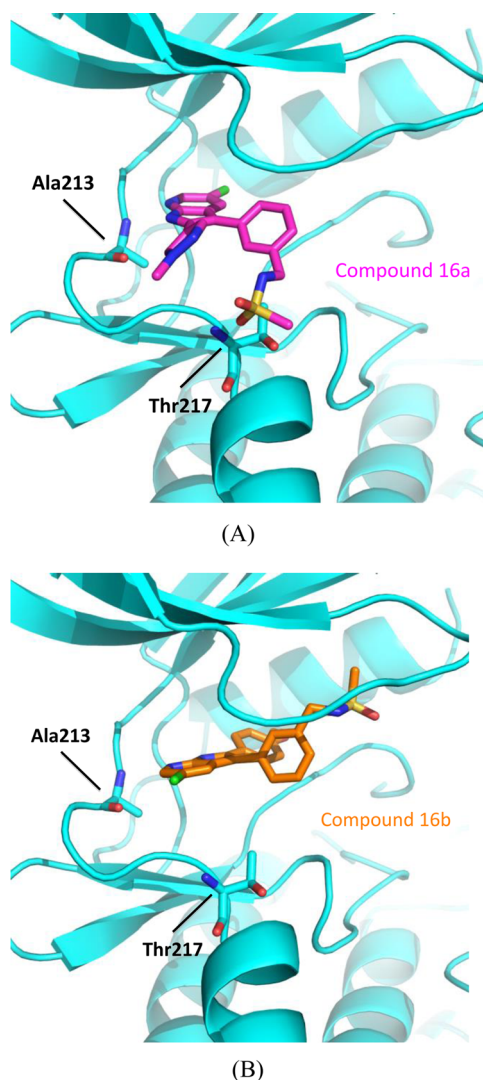
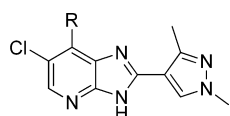


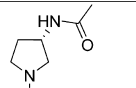
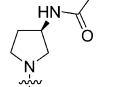
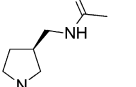
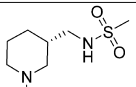
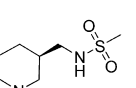
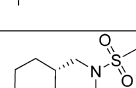
Figure 5. (A) Docking of **16a** into the active site of Aurora-A (PDB code 2X6D)²⁷ and (B) docking of **16b** into the active site of Aurora-A (PDB code 2X6D).²⁷

findings into account, we decided to terminate our interest in the 7-azindole scaffold and focus our efforts on evaluating the imidazo[4,5-*b*]pyridine-based approaches for Aurora-A-selective inhibition.

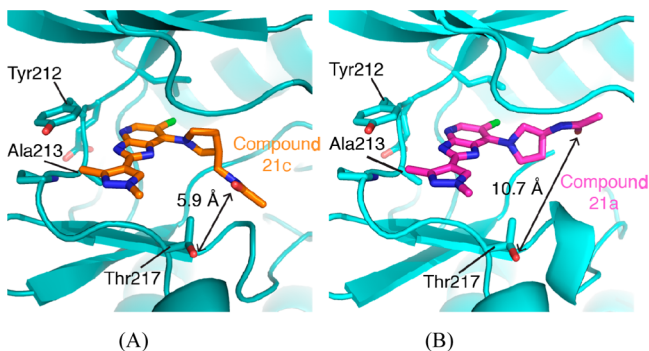
Targeting Aurora-A Thr217 for selective Aurora-A isoform inhibition was continued by investigation of C7-imidazo[4,5-*b*]pyridine derivatization, i.e., introduction of pyrrolidine- and piperidine-based substituents (Table 2). This approach afforded highly potent inhibitors of both Aurora-A and -B (**21a–f**, Table 2), with all compounds displaying similar inhibitory effects against these two Aurora isoforms. On this occasion, structural insight into ligand–protein interactions was gained by cocrystallization of **21c** and **21a** with Aurora-A. The complexes formed crystals in space group *P6₁22*, with one Aurora/compound complex per asymmetric unit.

Compound **21c** occupies the ATP-binding site, with the pyridine N and imidazole NH forming hydrogen bonds to Ala213 in the hinge region of Aurora-A consistent with previous reports (Figure 6A).^{27,28} The amide substituent of the pyrrolidine in **21c** points to Thr217 but is neither in the right orientation nor close enough (5.9 Å distance between the –OH of Thr217 and the amide carbonyl of compound **21c**) to form a

Table 2. C7-Imidazo[4,5-*b*]pyridine Derivatization: Pyrrolidine and Piperidine Substituents^a


| compound | R | Aurora-A IC ₅₀ , μM | Aurora-B IC ₅₀ , μM |
|----------|--|--------------------------------|--------------------------------|
| 21a |  | 0.27 ± 0.008 | 0.08 ± 0.018 |
| 21b |  | 0.004 ± 0.002 | 0.002 ± 0.001 |
| 21c |  | 0.009 ± 0.003 | 0.007 ^a |
| 21d |  | 0.005 ± 0.002 | 0.008 ± 0.002 |
| 21e |  | 0.007 ± 0.003 | 0.017 ± 0.007 |
| 21f |  | 0.005 ± 0.001 | 0.009 ± 0.001 |

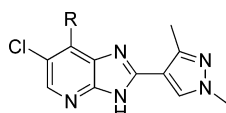
^aResults are mean values of two independent determinations (±SD) unless specified otherwise. A superscript Roman "a" indicates results from a single experiment (each concentration run in duplicate).

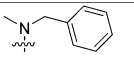
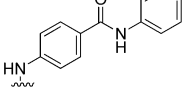
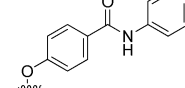
**Figure 6.** Crystal structures of C7-imidazo[4,5-*b*]pyridine compounds bound to Aurora-A: (A) compound 21c, (B) compound 21a.

strong hydrogen bond with the side chain of Thr217. Likewise, compound 21a binds to the hinge region as previously observed with closely related derivatives in this series. However, the substituted pyrrolidine ring adopts an unfavorable conformation for interaction with Thr217, with the acetamido group pointing away from this residue (Figure 6B). These crystal structures were consistent with the lack of selectivity for compounds 21a and 21c, and we therefore, investigated alternative substitutions at C7.

We continued our attempts to target Thr217 for Aurora-A-selective inhibition via C7-imidazo[4,5-*b*]pyridine derivatization by the introduction of a benzylamino substituent (compound

28a, Table 3) and 4-amino-*N*-phenylbenzamide substituent (compound 28b, Table 3). The benzylamino derivative 28a

Table 3. C7-Imidazo[4,5-*b*]pyridine Derivatization: Benzylamino, Anilino, and Phenoxy Substituents^a


| compound | R | Aurora-A IC ₅₀ , μM | Aurora-B IC ₅₀ , μM |
|----------|---|--------------------------------|--------------------------------|
| 28a |  | 0.255 ± 0.071 | 0.169 ^a |
| 28b |  | 0.075 ± 0.039 | 4.123 ± 1.584 |
| 28c |  | 0.067 ± 0.029 | 12.71 ± 10.99 |

^aThe results are mean values of at least two independent determinations (±SD) unless specified otherwise. A superscript Roman "a" indicates results from a single experiment (each concentration run in duplicate).

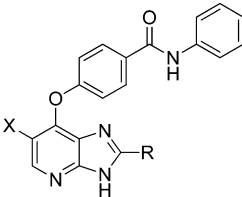
inhibited Aurora-A and -B with similar IC₅₀ values (Table 3). However, the *N*-phenylbenzamide derivative 28b was a significantly more potent inhibitor of Aurora-A compared to Aurora-B, the IC₅₀ values were determined as 0.075 and 4.12 μM, respectively (Table 3). A similar trend was observed in HeLa cervical cancer cells; 28b inhibited the autophosphorylation of Aurora-A at T288 (a cell-based biomarker for Aurora-A inhibition)^{17,19} with an IC₅₀ value of 0.32 μM and histone H3 phosphorylation at S10 (a cell-based biomarker for Aurora-B inhibition)^{17,19} with a significantly higher IC₅₀ value of 18.6 μM (58-fold difference). Subsequent replacement of the C7-NH linker in 28b with an oxygen gave compound 28c, which displayed a higher degree of selectivity in inhibiting Aurora-A over Aurora-B in biochemical assays (Table 3) and in cells. In the biochemical assays, the IC₅₀ values for inhibition of Aurora-A and -B were determined as 0.067 and 12.71 μM, respectively (Table 3). In HeLa cervical cancer cells, 28c inhibited the autophosphorylation of Aurora-A at T288 (p-T288 IC₅₀ = 0.16 μM) 480-fold more potently compared with Aurora-B inhibition (p-HH3 IC₅₀ = 76.84 μM). A similar trend was also observed in HCT116 human colon carcinoma cells; the IC₅₀ values for the inhibition of autophosphorylation of Aurora-A at T288 and histone H3 phosphorylation at S10 were determined as 0.065 and 24.65 μM, respectively. The selectivity of 28c against the kinome was also determined by profiling in a 110-kinase panel at a concentration of 1 μM. In this panel, 28c inhibited only three kinases at a level higher than 80%, namely, Aurora-A, VEGFR (VEGFR1), and GSK3b (Table S3, Supporting Information). On this basis, compound 28c is a highly selective kinase inhibitor with a Gini coefficient³⁷ calculated as 0.719. In an attempt to understand possible reasons for the observed inhibition of VEGFR1 and GSK3b by 28c, we examined conserved residues in the binding site between Aurora-A and VEGFR1 and between Aurora-A and GSK3b. We identified E211, Y212, G216, and L263 (residue numbers for Aurora-A) as conserved binding motifs between Aurora-A and VEGFR1 and residues L210, Y212, P214, and

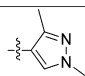
T217 (residue numbers for Aurora-A) as conserved binding motifs between Aurora-A and GSK3b. However, determination of whether these conserved regions influence the inhibition of VEGFR1 and GSK3b would require additional crystallography beyond the scope of this study. The antiproliferative activity in human tumor cell lines was also studied, and **28c** inhibited the growth of HCT116 human colon carcinoma cells with a GI_{50} value of $2.30 \mu\text{M}$. We have previously shown that compounds of the imidazo[4,5-*b*]pyridine class exhibit potent dual Aurora-A/FLT3 inhibition,²⁸ and consistent with this finding, we observed FLT3 inhibition in vitro ($IC_{50} = 0.162 \mu\text{M}$)³⁸ and potent antiproliferative activity in MV4-11 human AML cells ($GI_{50} = 0.299 \mu\text{M}$).

Compound **28c** displayed high mouse and liver microsomal stability (after a 30 min incubation with mouse and human liver microsomes, only 22% and 9% of **28c** was metabolized, respectively). This promising stability prompted in vivo mouse pharmacokinetic profiling that revealed **28c** as a highly orally bioavailable compound ($F = 100\%$) with moderate clearance (0.053 L/h , 44.16 mL/min/kg) and volume of distribution (0.036 L , 1.8 L/kg).

The effects of the 6-Cl and C2-pyrazolyl substituents on Aurora-A inhibition were subsequently studied by preparing compounds **34** and **35**, respectively (Scheme 8, Table 4). Both

Table 4. C6-Cl and C2-Pyrazolyl Aurora-A Inhibitory Effect^a



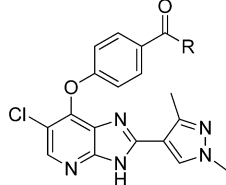
| compound | X | R | Aurora-A IC_{50} , μM |
|-----------|----|---|------------------------------------|
| 34 | H |  | 0.618 ± 0.215 |
| 35 | Cl | H | 25.84 ± 29.36 |

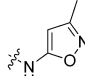
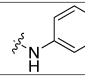
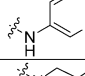
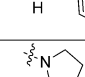
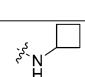
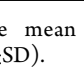
^aThe results are mean values of two independent determinations ($\pm\text{SD}$).

34 and **35** were significantly less potent inhibitors of Aurora-A compared to **28c** (Tables 3 and 4), indicating the requirement for both C6-Cl and C2-aromatic or -heteroaromatic substituents and consistent with previously reported SARs.^{27,28,39}

Having identified **28c** as a highly selective Aurora-A inhibitor, our efforts focused on replacing the aniline moiety in **28c**, a potential toxicophore,^{40,41} with a range of aliphatic and heteroaryl amines (Table 5). All replacements were well tolerated in relation to Aurora-A inhibitory potency, and the selectivity for Aurora-A over Aurora-B inhibition was generally maintained (Table 5). Compounds were also tested for the cellular inhibition of both Aurora-A and -B, and **40a** inhibited Aurora-A in HCT116 cells significantly more potently compared to Aurora-B (p-T288 $IC_{50} = 0.095 \mu\text{M}$ versus p-HH3 $IC_{50} = 4.93 \mu\text{M}$, 52-fold difference). Likewise, **40c** was a more potent inhibitor of Aurora-A than Aurora-B in Hela cells (p-T288 $IC_{50} = 0.28 \mu\text{M}$ versus p-HH3 $IC_{50} = 19.72 \mu\text{M}$, 70-fold difference). A similar trend was seen with **40b**; in Hela cells it inhibited Aurora-A more potently compared to Aurora-B (p-T288 $IC_{50} = 0.58 \mu\text{M}$

Table 5. Aniline Replacements^a



| compound | R | Aurora-A IC_{50} , μM | Aurora-B IC_{50} , μM |
|------------|---|------------------------------------|------------------------------------|
| 40a |  | 0.071 ± 0.008 | 0.693 ± 0.390 |
| 40b |  | 0.190 ± 0.071 | 3.447 ± 1.592 |
| 40c |  | 0.058 ± 0.034 | 1.676 ± 0.706 |
| 40d |  | 0.204 ± 0.122 | 3.910 ± 2.234 |
| 40e |  | 0.045 ± 0.012 | 1.817 ± 0.556 |
| 40f |  | 0.015 ± 0.006 | 3.045 ± 2.041 |

^aThe results are mean values of at least two independent determinations ($\pm\text{SD}$).

versus p-HH3 $IC_{50} = 19.74 \mu\text{M}$, 34-fold difference). Compound **40f** displayed the highest potency inhibiting Aurora-A in the biochemical assay ($IC_{50} = 0.015 \mu\text{M}$, Table 5), with Aurora-B inhibition being determined as $3.05 \mu\text{M}$ (Table 5). In Hela cells, **40f** inhibited Aurora-A 346 times more potently compared to Aurora-B (p-T288 $IC_{50} = 0.070 \mu\text{M}$ versus p-HH3 $IC_{50} = 24.24 \mu\text{M}$). Profiling of **40f** in a 50-kinase panel at a concentration of $1 \mu\text{M}$ revealed a highly selective inhibitor; only one kinase, namely, VEGFR (VEGFR1), was inhibited higher than 80% (Table S4, Supporting Information). Compound **40f** exhibited high mouse and liver microsomal stability (after a 30 min incubation with mouse and human liver microsomes, 28% and 22% of **40f** was metabolized, respectively). However, an in vivo pharmacokinetic profiling in mouse revealed a lower oral bioavailability (14%) compared to that for **28c** (100%).

Many attempts to cocrystallize **28c** and **40f** with Aurora-A were unsuccessful. However, the docking of **28c** into the active site of Aurora-A suggested that the aniline moiety resides in close proximity to Thr217 (Figure 4). On this basis, we probed whether Thr217 (Glu in Aurora-B) is the main residue governing the selectivity for Aurora-A inhibition. Testing of **28c** against the Aurora-A wild type and its T217E mutant expressed in Hela cells revealed that the Aurora-A T217E mutant was significantly less sensitive to inhibition (40-fold) compared to the Aurora-A wild type (p-T288 $IC_{50} = 4.11$ and $0.107 \mu\text{M}$, respectively). Subsequently, both **28c** and **40f** were tested against the Aurora-A wild type and its T217E, L215R, and R220K mutants in HCT116 cells (Table 6, Figure 7, and Figure S1 in the Supporting Information). Both **28c** and **40f** inhibited the Aurora-A L215R and R220K mutants with IC_{50} values similar to those seen for the Aurora-A wild type (Table 6, Figure 7, and Figure S1). On the other hand, the Aurora-A T217E mutant was significantly less sensitive to inhibition by **28c** and **40f** compared to the wild type (33-fold and 64-fold, respectively; Table 6,

Table 6. Inhibition of the Aurora-A Wild Type and Mutants in HCT116 Cells

| compd | Aur-A, WT p-T288 IC ₅₀ (μM) | Aur-A T217E mutant, p-T288 IC ₅₀ (μM) | Aur-A L215R mutant, p-T288 IC ₅₀ (μM) | Aur-A R220K mutant, p-T288 IC ₅₀ (μM) |
|-------|--|--|--|--|
| 28c | 0.029 | 0.96 | 0.027 | 0.027 |
| 40f | 0.036 | 2.29 | 0.043 | 0.042 |

Figure 7, and Figure S1). This body of evidence suggests that the Thr217 residue (Glu in Aurora-B/C) plays an important role in governing the observed selectivity for Aurora-A inhibition. In the above experiment, the inhibition of Aurora-B by **40f** was also investigated by measuring the reduction in the phosphorylation of histone H3 at S10. As shown in Figure S2 (Supporting Information), inhibition of histone H3 phosphorylation at S10 was only achieved at high concentrations of **40f** (partial inhibition at 25 μM and complete inhibition at 50 μM). Interestingly, at concentrations where phosphorylation of Aurora-A was completely inhibited (for example, at 1.5 μM), there was an increase in histone H3 phosphorylation (Figure S2), most likely due to an increase in the percentage of mitotic cells as previously reported for other Aurora-A-selective inhibitors.^{17,42} However, at higher concentrations, histone H3 phosphorylation was inhibited, indicating onset of Aurora B inhibition (Figure S2).

In conclusion, structural knowledge of imidazo[4,5-*b*]pyridine and imidazo[1,2-*a*]pyrazine-based ligand–Aurora-A protein interactions formed the basis of a design principle for imidazo[4,5-*b*]pyridine-derived Aurora-A-selective inhibition. This led to the discovery of imidazo[4,5-*b*]pyridine derivatives displaying a high degree of selectivity for inhibition of Aurora-A over Aurora-B in both biochemical and cellular assays. In particular, **28c** and **40f** were highly selective in inhibiting Aurora-A in both HeLa cervical cancer and HCT116 human colon carcinoma cells. Testing of **28c** and **40f** against the Aurora-A wild type and its T217E, L215R, and R220K mutants suggested that the Aurora-A Thr217 residue (Glu in Aurora-B/C) plays an important role in governing the observed selectivity for Aurora-A inhibition. In addition, **28c** and **40f** are a different chemotype compared to other known Aurora-A-selective inhibitors, and **28c** is highly selective within the tested kinome, with a kinase profiling differing from that of MK-5108⁴² and MLN8237.⁴³

These compounds could therefore serve as useful small-molecule tools^{44,45} to further explore the function of Aurora-A in cells; indeed, the need for structurally diverse inhibitors displaying Aurora isoform selectivity has recently been highlighted by Brockmann et al.²⁶ In their study, the Aurora-A-selective inhibitors MLN8054 and MLN8237 disrupted the Aurora-A/N-Myc complex and induced apoptosis in neuroblastoma cell lines and tumors, a phenotype different from that seen with the structurally differentiated Aurora-A-selective inhibitor MK-5108 from a different chemotype.²⁶ These data suggest differences in the mechanism of action and also indicate a specific target patient population for treatment with an Aurora-A-selective inhibitor.

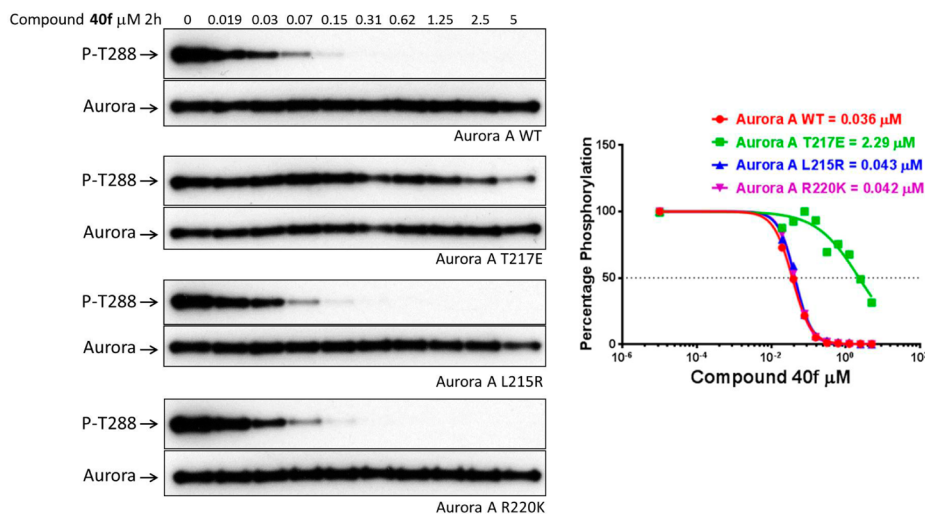
■ EXPERIMENTAL SECTION

Aurora Kinase Assays. Aurora-A and Aurora-B kinase IC₅₀ values were determined as follows: Kinase activity was measured in a microfluidic assay which monitors the separation of a phosphorylated product from its substrate. The assay was performed on an EZ Reader II (PerkinElmer Life Sciences, Waltham, MA) using separation buffer (no. 760367, PerkinElmer Life Sciences) containing CR-8 (500 nM, no. 760278, PerkinElmer Life Sciences). For each compound, a 10 mM stock concentration in 100% DMSO was used. Compounds were dispensed with an ECHO 550 acoustic dispenser (Labcyte Inc., Sunnyvale, CA) to generate duplicate 8 pt dilution curves directly into 384 LV polystyrene plates (no. 3676, Corning Inc., Corning, NY) to give final assay concentrations in the range of 0.25 pM to 200 μM in either 1.0% or 2% (v/v) DMSO.

For the Aurora-A kinase the enzyme reaction (total volume 10 μL) was carried out with 5 nM N-terminal HIS-tagged AurA, which was expressed and purified as previously described,⁴⁶ 1.5 μM fluorescently labeled peptide (no. 760365, FL-Peptide 21, PerkinElmer, sequence SFAM-LRRASLG-CONH₂), 20 μM ATP in assay buffer (50 mM Tris (pH 7.4), 200 mM NaCl, 5 mM MgCl₂, 2 mM DTT, 0.1% Tween 20), and the test compound or DMSO control.

For the Aurora-B kinase the enzyme reaction (total volume 10 μL) was carried out with 1 nM full-length AurB/INCENP complex (no. 05-102, Carina Biosciences, Inc., Kobe, Japan), 1.5 μM fluorescently labeled peptide (no. 760365, FL-Peptide 21, PerkinElmer, sequence SFAM-LRRASLG-CONH₂), 15 μM ATP in assay buffer (50 mM Tris (pH 7.4), 200 mM NaCl, 5 mM MgCl₂, 2 mM DTT, 0.1% Tween 20), and either the test compound or a DMSO control.

For both enzymes the reaction was carried out for 60 min at room temperature and stopped by the addition of 10 μL of stop buffer containing 100 mM HEPES-buffered saline (pH 7.3), 20 mM EDTA, and 0.05% (v/v) Brij-35. The plate was read on a Caliper EZ reader II.

**Figure 7.** Inhibition of Aurora-A wild-type and mutant proteins expressed in HCT116 cells by compound **40f**.

The reader provides a software package ("Reviewer") which converts the peak heights into percent conversion by measuring both product and substrate peaks. The percent inhibition was calculated relative to the total wells (containing enzyme) and blank wells (containing no enzyme plus DMSO). IC_{50} values were calculated from a four-parameter logistics fit of percentage inhibition versus log concentration using GraphPad Prism 5 (GraphPad Software, Inc., La Jolla, CA) or the Studies package (Dotmatics, Bishops Stortford, U.K.).

Kinase Selectivity Profiling. Compound **28c** was profiled against a panel of 110 kinases at the International Centre for Protein Kinase Profiling, Division of Signal Transduction Therapy, University of Dundee. Compound **40f** was profiled against a panel of 50 kinases (MRC-PPU Express Screen) also at the International Centre for Protein Kinase Profiling.

Cell Viability Assay. GI_{50} values (50% cell growth inhibitory concentration) were determined as previously described.^{27,47}

Inhibition of Aurora-B and the Aurora-A Wild Type and Mutants in Cells. Determination of cellular inhibition of Aurora-A (at T288) and histone H3 (at S10) has been described previously.¹⁹ Briefly, cells were transfected with the Myc-tagged Aurora-A wild type or mutants and treated with different concentrations of the inhibitors for 2 h followed by lysis in LDS sample buffer. The samples were sonicated and boiled, and the proteins were separated by LDS-PAGE and transferred to nitrocellulose membranes. The upper and lower parts of the membranes were probed with anti-P-T288 (Aurora-A autophosphorylation/activation) and anti-P-histone H3 (Aurora-B substrate phosphorylation) antibodies, respectively. The blots were quantified and IC_{50} values determined using Graphpad Prism. Mammalian cell expression constructs encoding Aurora-A T217E, L215R, and R220K mutants with N-terminal Myc tags were produced using Quikchange mutagenesis (Stratagene).

Computational Chemistry. The protein–ligand cocrystal (PDB 2X6D) was prepared in MOE (Molecular Operating Environment) using Protonate3D, and the waters were removed.⁴⁸ GOLD (Genetic Optimization for Ligand Docking) was used for all docking experiments using the ChemScore (chemscore_kinase) scoring function.⁴⁹ The docked poses were analyzed on the basis of their ChemScore and also the consistency of the docked poses. The higher scored poses were selected as the preferred solutions if the majority of these solutions were consistent in binding mode. The binding site was defined as those atoms within 6 Å of the cocrystallized ligand in PDB 2X6D and the cocrystal ligand removed. The GOLD algorithm was set to explore an extensive binding mode space by setting the *search efficiency* to 200%, or *very flexible*. No constraints were used in the docking experiments.

Cocrystallization of Aurora-A with Ligand. Cocrystals of Aurora-A bound to compounds **21a** and **21c** were generated as previously described.²⁸ Data were integrated using XDS and processed using the CCP4 package.⁵⁰ Structures were solved by molecular replacement using Aurora-A (PDB code 1MQ4) as a model. Ligand fitting and model rebuilding were carried out using Coot,⁵⁰ and refinement was carried out using Phenix.⁵¹

Mouse Liver Microsomal Stability. The compounds (10 μ M) were incubated with male CD1 mouse liver microsome (1 mg mL⁻¹) protein in the presence of NADPH (1 mM), UDPGA (2.5 mM), and MgCl₂ (3 mM) in phosphate-buffered saline (10 mM) at 37 °C. Incubations were conducted for 0 and 30 min. Control incubations were generated by the omission of NADPH and UDPGA from the incubation reaction. The percentage of compound remaining was determined after analysis by LC/MS.

Human Liver Microsomal Stability. The compounds (10 μ M) were incubated with mixed-gender pooled human liver microsome (1 mg mL⁻¹) protein in the presence of NADPH (1 mM), UDPGA (2.5 mM), and MgCl₂ (3 mM) in phosphate-buffered saline (10 mM) at 37 °C. Incubations were conducted for 0 and 30 min. Control incubations were generated by the omission of NADPH and UDPGA from the incubation reaction. The percentage of compound remaining was determined after analysis by LC/MS.

In Vivo Mouse PK (Compound 28c). Mice (female Balb/C) were dosed po or iv with **28c** (5 mg kg⁻¹) in 10% DMSO and 5% Tween 20 in saline. After administration, the mice were sacrificed at 5, 15, and 30 min

and 1, 2, 4, 6, and 24 h. Blood was removed by cardiac puncture and centrifuged to obtain plasma samples. The plasma samples (100 μ L) were added to the analytical internal standard (IS; olomoucine), followed by protein precipitation with 300 μ L of methanol. Following centrifugation (1200g, 30 min, 4 °C), the resulting supernatants were analyzed for **28c** levels by LC/MS using a reversed-phase X-Bridge C18 (Waters, 50 \times 2.1 mm) analytical column and positive ion mode ESI MRM on a Waters 2795 liquid chromatography system coupled to a Quattro Ultima triple-quadrupole mass spectrometer (Waters).

In Vivo Mouse PK (Compound 40f). Mice (female Balb/C) were dosed po or iv with **40f** (5 mg kg⁻¹) in 10% DMSO and 5% Tween 20 in saline. After administration, the mice were sacrificed at 5, 15, and 30 min and 1, 2, 4, 6, and 24 h. Blood was removed by cardiac puncture and centrifuged to obtain plasma samples. The plasma samples (100 μ L) were added to the analytical IS (olomoucine), followed by protein precipitation with 300 μ L of methanol. Following centrifugation (1200g, 30 min, 4 °C), the resulting supernatants were analyzed for **40f** levels by LC/MS using a reversed-phase Polar RP (Phenomenex, 50 \times 2 mm) analytical column and positive ion mode ESI MRM on a Waters 2795 liquid chromatography system coupled to a Quattro Ultima triple-quadrupole mass spectrometer (Waters).

Chemistry. General Procedures. Commercially available starting materials, reagents, and dry solvents were used as supplied.

Flash column chromatography was performed using Merck silica gel 60 (0.025–0.04 mm). Column chromatography was also performed on a FlashMaster personal unit using Isolute Flash silica columns or a Biotage SP1 purification system using Biotage Flash silica cartridges. Preparative TLC was performed on Analtech or Merck plates. Ion exchange chromatography was performed using acidic Isolute Flash SCX-II cartridges.

¹H NMR spectra were recorded on a Bruker Avance-500. Samples were prepared as solutions in a deuterated solvent and referenced to the appropriate internal nondeuterated solvent peak or tetramethylsilane. Chemical shifts were recorded in parts per million (δ) downfield of tetramethylsilane.

LC/MS analysis, method A: Analysis was performed on a Waters LCT with a Waters Alliance 2795 separation module and Waters 2487 dual-wavelength absorbance detector coupled to a Waters/Micromass LCT time-of-flight mass spectrometer with an ESI source. Analytical separation was carried out at 30 °C on a Merck Chromolith SpeedROD column (RP-18e, 50 \times 4.6 mm) using a flow rate of 2 mL/min in a 3.5 min gradient elution with detection at 254 nm. The mobile phase was a mixture of methanol (solvent A) and water containing formic acid at 0.1% (solvent B). Gradient elution was 1:9 (A/B) to 9:1 (A/B) over 2.25 min, 9:1 (A/B) for 0.75 min, then reversion back to 1:9 (A/B) over 0.3 min, and finally 1:9 (A/B) for 0.2 min. LC/MS analysis, method B: Analysis was performed on an Agilent 1200 series HPLC instrument with a diode array detector coupled to a 6210 time-of-flight mass spectrometer with a dual multimode APCI/ESI source. Analytical separation was carried out at 30 °C on a Merck Chromolith SpeedROD column (RP-18e, 50 \times 4.6 mm) using a flow rate of 2 mL/min in a 4 min gradient elution with detection at 254 nm. The mobile phase was a mixture of methanol (solvent A) and water containing formic acid at 0.1% (solvent B). Gradient elution was 1:9 (A/B) to 9:1 (A/B) over 2.5 min, 9:1 (A/B) for 1 min, then reversion back to 1:9 (A/B) over 0.3 min, and finally 1:9 (A/B) for 0.2 min. For LC/MS analyses, if the method is not stated, then method A was followed.

LC/HRMS analysis was performed on an Agilent 1200 series HPLC instrument with a diode array detector coupled to a 6210 time-of-flight mass spectrometer with a dual multimode APCI/ESI source. Analytical separation was carried out at 30 °C on a Merck Chromolith SpeedROD column (RP-18e, 50 \times 4.6 mm) using a flow rate of 2 mL/min in a 4 min gradient elution with detection at 254 nm. The mobile phase was a mixture of methanol (solvent A) and water containing formic acid at 0.1% (solvent B). Gradient elution was 1:9 (A/B) to 9:1 (A/B) over 2.5 min, 9:1 (A/B) for 1 min, then reversion back to 1:9 (A/B) over 0.3 min, and finally 1:9 (A/B) for 0.2 min. The following references masses were used for HRMS analysis: caffeine [M + H]⁺ 195.087652, (hexakis-(1H,1H,3H-tetrafluoropentoxy)phosphazene [M + H]⁺ 922.009798),

and hexakis(2,2-difluoroethoxy)phosphazene $[M + H]^+$ 622.02896 or reserpine $[M + H]^+$ 609.280657.

Analytical HPLC analysis was performed on a Thermo-Finnigan Surveyor HPLC system or an Agilent Technologies 1200 series HPLC system at 30 °C using a Phenomenex Gemini C₁₈ column (5 μm, 50 × 4.6 mm) and 10 min gradient of 10% → 90% MeOH/0.1% formic acid, visualizing at 254, 309, or 350 nm. The purity of the final compounds was determined by analytical HPLC as described above and is ≥95% unless specified otherwise.

(S)-*N*-(1-(2-Amino-5-chloro-3-nitropyridin-4-yl)pyrrolidin-3-yl)acetamide (**20a**). To a mixture of 4,5-dichloro-3-nitropyridin-2-amine (0.152 g, 0.73 mmol) and 2-propanol (13.0 mL) was added *(S)*-3-acetamidopyrrolidine (0.098 g, 0.77 mmol) followed by *N,N*-diisopropylethylamine (0.17 mL, 0.97 mmol). The reaction mixture was placed in an oil bath preheated at 45 °C and stirred at this temperature for 18 h; it was then allowed to cool to room temperature and diluted with 2-propanol (8 mL). The precipitate was collected by filtration, washed with 2-propanol (2 × 5 mL) and diethyl ether (5 mL), and dried to give the title compound as a yellow solid (0.133 g, 61%): ¹H NMR (500 MHz, DMSO-*d*₆) 1.80 (s, 3H, COCH₃), 1.83 (m, 1H, pyrrolidine CH), 2.08 (m, 1H, pyrrolidine CH), 3.18 (dd, *J* = 5.1, 10.5 Hz, 1H, pyrrolidine CH), 3.56 (m, 2H, pyrrolidine CH), 3.64 (m, 1H, pyrrolidine CH), 4.20 (m, 1H, pyrrolidine CH), 6.85 (s, 2H, NH₂), 7.88 (s, 1H, pyridine 6-H), 8.09 (d, *J* = 6.1 Hz, 1H, CONH); LC/MS (ESI, *m/z*) *t*_R = 1.32 min, 300, 302 [(*M* + *H*)⁺, Cl isotopic pattern].

(S)-*N*-(1-(6-Chloro-2-(1,3-dimethyl-1H-pyrazol-4-yl)-3H-imidazo[4,5-*b*]pyridin-7-yl)pyrrolidin-3-yl)acetamide (**21a**). To a mixture of *(S)*-*N*-(1-(2-amino-5-chloro-3-nitropyridin-4-yl)pyrrolidin-3-yl)acetamide (0.045 g, 0.15 mmol) and ethanol (3.5 mL) was added 1,3-dimethyl-1H-pyrazole-4-carbaldehyde (0.020 g, 0.16 mmol) followed by a freshly prepared aqueous solution of Na₂S₂O₄ (1 M, 0.65 mL, 0.65 mmol). The reaction mixture was stirred at 80 °C for 20 h; it was then concentrated in vacuo. The residue was absorbed on silica gel (1.7 g), and the free-running powder was placed on a 10 g Isolute silica column. Elution with dichloromethane/ethyl acetate (1:1, v/v), 4% methanol in dichloromethane/ethyl acetate (1:1, v/v), and 6% methanol in dichloromethane/ethyl acetate (1:1, v/v) afforded a solid residue which was triturated with diethyl ether. The precipitate was collected by filtration and washed with diethyl ether, water (4 × 2 mL), and diethyl ether (3 × 3 mL) to afford the title compound as a pale yellow solid (0.022 g, 39%): ¹H NMR (500 MHz, DMSO-*d*₆) 1.81 (s, 3H, COCH₃), 1.85 (m, 1H, pyrrolidine CH), 2.08 (m, 1H, pyrrolidine CH), 3.83 (s, 3H, pyrazole *N*-CH₃), 3.92 (m, 1H, pyrrolidine CH), 4.16 (m, 1H, pyrrolidine CH), 4.25 (m, 3H, pyrrolidine CH), 7.86 (s, 1H) and 8.12 (s, 2H) (pyrazole 5-H, imidazo[4,5-*b*]pyridine 5-H and CONH), 12.78 (s, 1H, imidazo[4,5-*b*]pyridine NH); LC/MS (ESI, *m/z*) *t*_R = 1.90 min, 374, 376 [(*M* + *H*)⁺, Cl isotopic pattern]; HRMS *m/z* found 374.1496, calcd for C₁₇H₂₁ClN₇O (*M* + *H*)⁺ 374.1491; HPLC *t*_R = 6.18 min, 94% at λ = 354 nm.

(S)-*tert*-Butyl 3-(Acetamidomethyl)pyrrolidine-1-carboxylate (**23**). To a solution of *(S)*-*tert*-butyl 3-(aminomethyl)pyrrolidine-1-carboxylate (0.30 g, 1.50 mmol) in anhydrous CH₂Cl₂ (4 mL) cooled in an ice bath under argon was added DIPEA (0.213 g, 0.29 mL, 1.65 mmol) followed by a dropwise addition of acetic anhydride (0.168 g, 1.65 mmol). The reaction mixture was stirred for 4 h under argon while being allowed to warm to room temperature. The clear solution was diluted with ethyl acetate (50 mL), washed with saturated NaHCO₃ (20 mL), brine (20 mL), 1 M aq HCl (20 mL), and brine (20 mL), then dried (Na₂SO₄), and concentrated in vacuo. The product was obtained as a colorless oil (0.300 g, 83%): ¹H NMR (500 MHz, DMSO-*d*₆) 1.39 (s, 9H, C(CH₃)₃), 1.53 (m, 1H, pyrrolidine CH), 1.80 (s, 3H, COCH₃), 1.85 (m, 1H), 2.23 (m, 1H), 2.89 (dd, *J* = 7.2, 10.8 Hz, 1H), 3.00 (m, 1H), 3.07 (m, 1H), 3.16 (m, 1H), and 3.32 (m, obscured by water peak) (pyrrolidine CH and CH₂NH), 7.89 (s, 1H, CONH); LC/MS (ESI, *m/z*) compound is non-UV-absorbent, 265 (*M* + *Na*)⁺.

(S)-*N*-(1-(2-Amino-5-chloro-3-nitropyridin-4-yl)pyrrolidin-3-yl)methyl)acetamide (**20c**). A solution of *(S)*-*tert*-butyl 3-(acetamidomethyl)pyrrolidine-1-carboxylate (0.263 g, 1.09 mmol) in dichloromethane (7 mL) and trifluoroacetic acid (3.0 mL) was stirred at room temperature for 1.5 h. Solvents were removed in vacuo and

azeotroped with toluene to leave a colorless oily residue, (*R*)-*N*-(pyrrolidin-3-ylmethyl)acetamide as a TFA salt. This material (supposedly 1.08 mmol) was dissolved in 2-propanol (14 mL), and to this solution was added 4,5-dichloro-3-nitropyridin-2-amine (0.214 g, 1.03 mmol) followed by *N,N*-diisopropylethylamine (0.503 g, 0.68 mL, 3.89 mmol). The reaction mixture was placed into an oil bath preheated to 45 °C and stirred at this temperature for 20 h; a nearly clear solution was obtained. Approximately half of the solvent volume was then removed in vacuo to give a precipitate which was collected by filtration and washed with 2-propanol and diethyl ether. The product was obtained as a yellow solid (0.205 g, 64%): ¹H NMR (500 MHz, DMSO-*d*₆) 1.62 (m, 1H, pyrrolidine CH), 1.79 (s, 3H, COCH₃), 1.95 (m, 1H, pyrrolidine CH), 2.32 (m, 1H, pyrrolidine CH), 3.03 (m, 1H), 3.12 (m, 1H), 3.21 (dd, *J* = 6.3, 10.4 Hz, 1H), and 3.38–3.52 (m, 3H) (pyrrolidine CH and CH₂NH), 6.84 (s, 2H, NH₂), 7.87 (s, 1H, pyridine 6-H), 7.93 (br t, *J* = 5.4 Hz, 1H, CONH); LC/MS (ESI, *m/z*) *t*_R = 1.26 min, 314, 316 [(*M* + *H*)⁺, Cl isotopic pattern].

(S)-*N*-((1-(6-Chloro-2-(1,3-dimethyl-1H-pyrazol-4-yl)-3H-imidazo[4,5-*b*]pyridin-7-yl)pyrrolidin-3-yl)methyl)acetamide (**21c**). To a mixture of *(S)*-*N*-((1-(2-amino-5-chloro-3-nitropyridin-4-yl)pyrrolidin-3-yl)methyl)acetamide (0.055 g, 0.18 mmol) and ethanol (3.5 mL) was added 1,3-dimethyl-1H-pyrazole-4-carbaldehyde (0.024 g, 0.19 mmol) followed by a freshly prepared aqueous solution of Na₂S₂O₄ (1 M, 0.75 mL, 0.75 mmol), and the reaction mixture was stirred at 80 °C for 20 h. The reaction mixture was then concentrated in vacuo, the residue was absorbed on silica gel (1.7 g), and the free-running powder was placed on a 10 g Isolute silica column which was eluted with dichloromethane/ethyl acetate (1:1, v/v), 5% methanol in dichloromethane/ethyl acetate (1:1, v/v), and 9% methanol in dichloromethane/ethyl acetate (1:1, v/v). Trituration of the resultant residue with diethyl ether gave a precipitate which was collected by filtration, washed with diethyl ether, water, and diethyl ether, and then dried. The title compound was obtained as an off-white solid (0.016 g, 23%): ¹H NMR (500 MHz, DMSO-*d*₆) 1.64 (m, 1H, pyrrolidine CH), 1.81 (s, 3H, COCH₃), 2.01 (m, 1H, pyrrolidine CH), 2.35 (m, 1H, pyrrolidine CH), 3.83 (s, 3H, pyrazole *N*-CH₃), 3.13 (t, *J* = 6.3 Hz, 2H), 3.85 (m, 1H), and 4.14 (m, 3H) (pyrrolidine CH and CH₂NH), 7.86 (s, 1H, pyrazole 5-H or imidazo[4,5-*b*]pyridine 5-H), 7.94 (br t, *J* = 5.1 Hz, 1H, CONH), 8.12 (s, 1H, imidazo[4,5-*b*]pyridine 5-H or pyrazole 5-H), 12.76 (s, 1H, imidazo[4,5-*b*]pyridine NH); LC/MS (ESI, *m/z*) *t*_R = 1.78 min, 388, 390 [(*M* + *H*)⁺, Cl isotopic pattern]; HRMS *m/z* found 388.1649, calcd for C₁₈H₂₃ClN₇O (*M* + *H*)⁺ 388.1647.

4-(2-Amino-5-chloro-3-nitropyridin-4-yl)amino)-*N*-phenylbenzamide (**29**). To a mixture of 4,5-dichloro-3-nitropyridin-2-amine (0.104 g, 0.50 mmol) and 2-propanol (7.0 mL) was added 4-aminobenzanilide (0.114 g, 0.54 mmol) followed by *N,N*-diisopropylethylamine (0.105 mL, 0.078 g, 0.60 mmol). The reaction mixture was heated at 45 °C for 18 h, then the temperature was raised to 90 °C, and stirring was continued at this temperature for 7 h. The reaction mixture was then allowed to cool to room temperature and diluted with 2-propanol (8.0 mL); a precipitate was obtained which was collected by filtration, washed with 2-propanol (2 × 5 mL) and diethyl ether (2 × 5 mL), and dried to afford the title compound as an orange solid (0.070 g, 37%): ¹H NMR (500 MHz, DMSO-*d*₆) 7.02 (d, *J* = 8.7 Hz, 2H, ArH), 7.08 (t, *J* = 7.2 Hz, 1H, *p*-PhH), 7.26 (s, 2H, NH₂), 7.33 (t, *J* = 8.3 Hz, 2H, *m*-PhH), 7.75 (d, *J* = 7.8 Hz, 2H, ArH), 7.86 (d, *J* = 8.7 Hz, 2H, ArH), 8.18 (s, 1H, pyridine 6-H), 9.14 (s, 1H, NHAr), 10.07 (s, 1H, NHAr); LC/MS (ESI, *m/z*) *t*_R = 2.31 min, 384, 386 [(*M* + *H*)⁺, Cl isotopic pattern].

4-(6-Chloro-2-(1,3-dimethyl-1H-pyrazol-4-yl)-3H-imidazo[4,5-*b*]pyridin-7-yl)amino)-*N*-phenylbenzamide (**28b**). To a mixture of 4-(2-amino-5-chloro-3-nitropyridin-4-yl)amino)-*N*-phenylbenzamide (0.065 g, 0.17 mmol) and ethanol (5.5 mL) was added 1,3-dimethyl-1H-pyrazole-4-carbaldehyde (0.024 g, 0.19 mmol) followed by a freshly prepared aqueous solution of Na₂S₂O₄ (1M; 0.90 mL, 0.90 mmol). The reaction mixture was stirred at 80 °C for 22 h, then allowed to cool to room temperature, and concentrated in vacuo. The residue was absorbed on silica gel (1.7 g), and the free-running powder was placed on a 10 g Isolute silica column which was eluted with CH₂Cl₂, dichloromethane/ethyl acetate (1:1, v/v), 2% methanol in dichloromethane/ethyl acetate (1:1, v/v), and finally 3% methanol in

dichloromethane/ethyl acetate (1:1, v/v). The title compound was obtained as an off-white solid after trituration with diethyl ether/CH₂Cl₂ (1:1, v/v) (0.012 g, 15%): ¹H NMR (500 MHz, DMSO-*d*₆) 2.22 (s, 3H, pyrazole 3-Me), 3.82 (s, 3H, pyrazole *N*-Me), 7.08 (t, *J* = 7.4 Hz, 1H, *p*-PhH), 7.19 (d, *J* = 7.2 Hz, 2H, ArH), 7.33 (t, *J* = 7.8 Hz, 2H, *m*-PhH), 7.78 (d, *J* = 7.9 Hz, 2H, ArH), 7.89 (d, *J* = 8.7 Hz, 2H, ArH), 8.16 (s, 1H, pyrazole 5-H or imidazo[4,5-*b*]pyridine 5-H), 8.17 (s, 1H, pyrazole 5-H or imidazo[4,5-*b*]pyridine 5-H), 8.74 (s, 1H, NHAr), 9.97 (s, 1H, NHAr), 13.03 (s, 1H, imidazo[4,5-*b*]pyridine NH); LC/MS (ESI, *m/z*) *t*_R = 2.36 min, 458, 460 [(*M* + *H*)⁺, Cl isotopic pattern]; HRMS *m/z* found 458.1493, calcd for C₂₄H₂₁ClN₇O (*M* + *H*)⁺ 458.1491.

4-((2-Amino-5-chloro-3-nitropyridin-4-yl)oxy)-*N*-phenylbenzamide (31). To a solution of 4-hydroxy-*N*-phenylbenzamide³⁴ (0.068g, 0.32 mmol) in anhydrous DMF (2.3 mL) was added potassium *tert*-butoxide (0.036 g, 0.32 mmol). The solution was stirred at room temperature for 20 min under argon, and then 4,5-dichloro-3-nitropyridin-2-amine (0.062 g, 0.30 mmol) was added portionwise over a 5 min period. Stirring was continued at room temperature for 1 h and 10 min under argon; the reaction mixture was then partitioned between ethyl acetate (110 mL) and H₂O (20 mL). The organic layer was washed with H₂O (15 mL) and brine (20 mL), dried (Na₂SO₄), and concentrated in vacuo to give a yellow solid. This was triturated with dichloromethane, the precipitate was collected by filtration and washed with dichloromethane to obtain the title compound as a yellow solid (0.087 g, 76%): ¹H NMR (500 MHz, DMSO-*d*₆) 7.09 (t, *J* = 7.4 Hz, 1H, *p*-PhH), 7.13 (d, *J* = 8.8 Hz, 2H, ArH), 7.34 (t, *J* = 7.7 Hz, 2H, *m*-PhH), 7.62 (br s, 2H, NH₂), 7.75 (d, *J* = 7.7 Hz, 2H, ArH), 7.95 (d, *J* = 8.8 Hz, 2H, ArH), 8.46 (s, 1H, pyridine 6-H), 10.24 (s, 1H, CONH); LC/MS (ESI, *m/z*) *t*_R = 2.50 min, 385, 387 [(*M* + *H*)⁺, Cl isotopic pattern].

4-((6-Chloro-2-(1,3-dimethyl-1H-pyrazol-4-yl)-3H-imidazo[4,5-*b*]pyridin-7-yl)oxy)-*N*-phenylbenzamide (28c). To a mixture of 4-((2-amino-5-chloro-3-nitropyridin-4-yl)oxy)-*N*-phenylbenzamide (0.077 g, 0.20 mmol) and DMF (4.2 mL) was added 1,3-dimethyl-1H-pyrazole-4-carbaldehyde (0.030 g, 0.24 mmol) followed by a freshly prepared aqueous solution of Na₂S₂O₄ (1 M, 1.0 mL, 1.0 mmol). The reaction mixture was stirred at 84 °C for 20 h, then allowed to cool to room temperature, and partitioned between EtOAc (180 mL) and water (20 mL). The organic layer washed with more H₂O (15 mL), and brine (15 mL), dried (Na₂SO₄), and concentrated in vacuo. The resulting residue was triturated with diethyl ether (15 mL); the precipitate was collected by filtration and washed with diethyl ether. This solid was absorbed on silica gel (1.4 g), and the free-running powder was placed on a 10 g Isolute silica column which was eluted with dichloromethane, dichloromethane/ethyl acetate (1:1, v/v), 2.5% methanol in dichloromethane/ethyl acetate (1:1, v/v), and finally 4% methanol in dichloromethane/ethyl acetate (1:1, v/v). The obtained residue was triturated with diethyl ether; the precipitate was collected by filtration and washed with diethyl ether to give the title compound as an off-white solid (0.010 g, 11%): ¹H NMR (500 MHz, DMSO-*d*₆) 2.21 (s, 3H, pyrazole 3-Me), 3.82 (s, 3H, pyrazole *N*-Me), 7.09 (t, *J* = 7.4 Hz, 1H, *p*-PhH), 7.18 (br d, *J* = 7.5 Hz, 2H, ArH), 7.34 (t, *J* = 7.8 Hz, 2H, *m*-PhH), 7.75 (d, *J* = 8.0 Hz, 2H, ArH), 7.98 (d, *J* = 8.8 Hz, 2H, ArH), 8.21 (br s, 1H, pyrazole 5-H or imidazo[4,5-*b*]pyridine 5-H), 8.38 (br s, 1H, pyrazole 5-H or imidazo[4,5-*b*]pyridine 5-H), 10.16 (s, 1H, CONH), 13.35 (s, 1H, imidazo[4,5-*b*]pyridine NH); LC/MS (ESI, *m/z*) *t*_R = 2.56 min, 459, 461 [(*M* + *H*)⁺, Cl isotopic pattern]; HRMS *m/z* found 459.1348, calcd for C₂₄H₂₀ClN₆O₂ (*M* + *H*)⁺ 459.1331.

4-(Cyclobutylcarbamoyl)phenyl Acetate (37f). To a round-bottom flask containing 4-acetoxybenzoic acid (0.306 g, 1.70 mmol) was slowly added a solution of oxalyl chloride (0.430 g, 3.40 mmol) in anhydrous dichloromethane (2.0 mL) under argon. To this mixture was slowly added anhydrous DMF (0.030 mL), and a clear solution was obtained. The solution was stirred at room temperature for 45 min under argon and then concentrated in vacuo, and the residue was dissolved in anhydrous dichloromethane (3.0 mL). Cyclobutylamine (0.363 g, 5.10 mmol) was slowly added; a precipitate had formed by completion of the amine addition. Stirring was continued at room temperature for 20 min. Then the reaction mixture was diluted with anhydrous dichloromethane (2.0 mL), and the precipitate was removed by filtration and washed with dichloromethane (4 × 3 mL). The filtrate was concentrated in vacuo and

absorbed on silica gel (1.6 g), and the free-running powder was placed on a 20 g Isolute silica column which eluted with dichloromethane and then 5%, 10%, and 15% EtOAc in dichloromethane. The obtained product was dissolved in EtOAc (150 mL), and the solution was washed with saturated aqueous NaHCO₃ (3 × 20 mL), dried (Na₂SO₄), and concentrated in vacuo to give the title compound as a white solid (0.150 g, 38%): ¹H NMR (500 MHz, DMSO-*d*₆) 1.66 (m, 2H, cyclobutylamine CH), 2.06 (m, 2H, cyclobutylamine CH), 2.20 (m, 2H, cyclobutylamine CH), 2.28 (s, 3H, COCH₃), 4.39 (m, 1H, NHCH), 7.20 (d, *J* = 8.6 Hz, 2H, ArH), 7.87 (d, *J* = 8.6 Hz, 2H, ArH), 8.57 (d, *J* = 7.4 Hz, 1H, CONH); LC/MS (ESI, *m/z*) *t*_R = 1.91 min, 234 (*M* + *H*)⁺.

***N*-Cyclobutyl-4-hydroxybenzamide (38f).** To a mixture of 4-(cyclobutylcarbamoyl)phenyl acetate (0.145 g, 0.62 mmol) in methanol (4.0 mL) was added an aqueous solution of NaOH (1M, 1.6 mL, 1.6 mmol) followed by water (0.4 mL); a clear solution was obtained. The reaction mixture was stirred at room temperature for 1 h and 20 min. Approximately half of the solvent was then removed under reduced pressure, and the remaining solution was diluted with water (2.0 mL). The pH was adjusted to about 7 with 1 M HCl; a white suspension was obtained which was diluted with water (5 mL). This was extracted with EtOAc (3 × 50 mL), and the combined extracts were dried (Na₂SO₄) and concentrated in vacuo to give the title compound as a white solid (0.105 g, 89%): ¹H NMR (500 MHz, DMSO-*d*₆) 1.67 (m, 2H, cyclobutylamine CH), 2.05 (m, 2H, cyclobutylamine CH), 2.18 (m, 2H, cyclobutylamine CH), 4.37 (m, 1H, NHCH), 6.77 (d, *J* = 8.7 Hz, 2H, ArH), 7.70 (d, *J* = 8.7 Hz, 2H, ArH), 8.28 (d, *J* = 7.5 Hz, 1H, CONH), 9.87 (s, 1H, OH); LC/MS (ESI, *m/z*) *t*_R = 1.66 min, 192 (*M* + *H*)⁺.

4-((2-Amino-5-chloro-3-nitropyridin-4-yl)oxy)-*N*-cyclobutylbenzamide (39f). To a solution of *N*-cyclobutyl-4-hydroxybenzamide (0.100 g, 0.52 mmol) in anhydrous DMF (3.3 mL) was added potassium *tert*-butoxide (0.058 g, 0.52 mmol). The solution was stirred at room temperature for 20 min under argon. Then 4,5-dichloro-3-nitropyridin-2-amine (0.102 g, 0.49 mmol) was added portionwise over a 5 min period. Stirring was continued at room temperature for 1 h and 30 min under argon; the reaction mixture was then partitioned between ethyl acetate (200 mL)/dichloromethane (5 mL) and H₂O (30 mL). The organic layer was washed with H₂O (20 mL), brine (30 mL), saturated aqueous NaHCO₃ (20 mL), and brine (20 mL), dried (Na₂SO₄), and concentrated in vacuo to give a yellow solid. This solid was triturated with EtOAc/dichloromethane (1:1, v/v; approximately 10 mL); the precipitate was collected by filtration and washed with dichloromethane to afford the title compound as a yellow solid (0.120 g, 67%): ¹H NMR (500 MHz, DMSO-*d*₆) 1.66 (m, 2H, cyclobutylamine CH), 2.05 (m, 2H, cyclobutylamine CH), 2.20 (m, 2H, cyclobutylamine CH), 4.38 (m, 1H, NHCH), 7.04 (d, *J* = 8.9 Hz, 2H, ArH), 7.54 (s, 2H, NH₂), 7.83 (d, *J* = 8.9 Hz, 2H, ArH), 8.43 (s, 1H, pyridine 6-H), 8.53 (d, *J* = 7.5 Hz, 1H, CONH); LC/MS (ESI, *m/z*) *t*_R = 2.31 min, 363, 365 [(*M* + *H*)⁺, Cl isotopic pattern].

4-((6-Chloro-2-(1,3-dimethyl-1H-pyrazol-4-yl)-3H-imidazo[4,5-*b*]pyridin-7-yl)oxy)-*N*-cyclobutylbenzamide (40f). To a mixture of 4-((2-amino-5-chloro-3-nitropyridin-4-yl)oxy)-*N*-cyclobutylbenzamide (0.094 g, 0.26 mmol) and DMF (5.9 mL) was added 1,3-dimethyl-1H-pyrazole-4-carbaldehyde (0.038 g, 0.31 mmol) followed by a freshly prepared aqueous solution of Na₂S₂O₄ (1 M, 1.3 mL, 1.30 mmol). The reaction mixture was stirred at 85 °C for 24 h, then allowed to cool to room temperature, and partitioned between EtOAc (220 mL) and water (30 mL). The organic layer was washed with more H₂O (20 mL) and brine (20 mL), dried (Na₂SO₄), and concentrated in vacuo. The residue was treated with diethyl ether (approximately 15 mL); a brown precipitate was obtained which was collected by filtration and washed with diethyl ether. This solid was absorbed on silica gel (1.2 g), and the free-running powder was placed on a 10 g Isolute silica column which was eluted with dichloromethane, dichloromethane/ethyl acetate (1:1, v/v), 2.5% methanol in dichloromethane/ethyl acetate (1:1, v/v), and finally 4% methanol in dichloromethane/ethyl acetate (1:1, v/v). The obtained residue was triturated with diethyl ether; the precipitate was collected by filtration and washed with diethyl ether to give the title compound as an off-white solid (0.016 g, 14%): ¹H NMR (500 MHz, DMSO-*d*₆) 1.67 (m, 2H, cyclobutylamine CH), 2.06 (m, 2H, cyclobutylamine CH), 2.19 (m, 5H, cyclobutylamine CH and pyrazole

3-Me), 3.82 (s, 3H, pyrazole N-Me), 4.40 (m, 1H, NHCH), 7.10 (d, $J = 8.1$ Hz, 2H, ArH), 7.85 (d, $J = 8.7$ Hz, 2H, ArH), 8.19 (s, 1H) and 8.34 (s, 1H) (pyrazole 5-H and imidazo[4,5-*b*]pyridine 5-H), 8.51 (d, $J = 7.2$ Hz, 1H, CONH), 13.31 (s, 1H, imidazo[4,5-*b*]pyridine NH); LC/MS (ESI, m/z) $t_R = 2.44$ min, 437, 439 [(M + H)⁺, Cl isotopic pattern]; HRMS m/z found 437.1492, calcd for C₂₂H₂₂ClN₆O₂ (M + H)⁺ 437.1487.

■ ASSOCIATED CONTENT

Supporting Information

Experimental procedures for compounds 9–15, 16a–d, 17, 20b,d–f, 21b,d–f, 25–27, 28a, 32–35, 37a,b,d,e, 38a,b,d,e, 39a–e, and 40a–e, summary of crystallographic analysis of compounds 21c (Table S1) and 21a (Table S2), kinase selectivity profiling of compounds 28c (Table S3) and 40f (Table S4), inhibition of the Aurora-A wild type and mutants in HCT116 cells by compound 28c (Figure S1), inhibition of Aurora-B in HCT116 cells by compound 40f (Figure S2), and omit electron density maps for compounds 21a,c (Figure S3). This material is available free of charge via the Internet at <http://pubs.acs.org>.

Accession Codes

Atomic coordinates and structure factors for the crystal structure of Aurora-A with compounds 21a and 21c can be accessed using PDB codes 4BYJ and 4BYI, respectively.

■ AUTHOR INFORMATION

Corresponding Authors

*Phone: +44 (0) 20 87224158. E-mail: vassilios.bavetsias@icr.ac.uk.

*Phone: +44 (0) 20 87224051. E-mail: julian.blagg@icr.ac.uk.

Notes

The authors declare the following competing financial interest(s): Please note that all authors who are, or have been, employed by The Institute of Cancer Research are subject to a “Rewards to Inventors Scheme” which may reward contributors to a program that is subsequently licensed. P.W. was a founder and shareholder in Chroma Therapeutics. P.W. is a former employee of AstraZeneca. J.B. is a former employee and shareholder of Pfizer Inc.

■ ACKNOWLEDGMENTS

This work was supported by Cancer Research UK [CUK] Grants C309/A8274 and C309/A11566. P.W. is a Cancer Research UK Life Fellow. S.L. is supported by Breakthrough Breast Cancer. R.B. is a Royal Society University Research Fellow and acknowledges the support of Breakthrough Breast Cancer Project Grant AURA 05/06 and Cancer Research UK Grant C24461/A13231 and infrastructural support for Structural Biology at The Institute of Cancer Research from Cancer Research UK. We acknowledge National Health Service (NHS) funding to the National Institute for Health Research (NIHR) Biomedical Research Centre at The Institute of Cancer Research and the Royal Marsden NHS Foundation Trust. We also thank Dr. Amin Mirza, Mr. Meirion Richards, Dr. Maggie Liu, and Dr. Charlotte Dodson for their assistance with NMR, mass spectrometry, HPLC, and Aurora-A protein production.

■ ABBREVIATIONS USED

Boc, *tert*-butoxycarbonyl; DABCO, 1,4-diazabicyclo[2,2,2]-octane; DIPEA, *N,N*-diisopropylethylamine; ESI, electrospray ionization; HPLC, high-performance liquid chromatography; HRMS, high-resolution mass spectrometry; LC, liquid chroma-

tography; SAR, structure–activity relationship; TFA, trifluoroacetic acid

■ REFERENCES

- (1) Pollard, J. R.; Mortimore, M. Discovery and Development of Aurora Kinase Inhibitors as Anticancer Agents. *J. Med. Chem.* **2009**, *52*, 2629–2651.
- (2) Green, M. R.; Woolery, J. E.; Mahadevan, D. Update on Aurora Kinase Targeted Therapeutics in Oncology. *Expert Opin. Drug Discovery* **2011**, *6*, 291–307.
- (3) Cheung, C. H. A.; Coumar, M. S.; Chang, J.-Y.; Hsieh, H.-P. Aurora Kinase Inhibitor Patents and Agents in Clinical Testing: An Update (2009–10). *Expert Opin. Ther. Patents* **2011**, *21*, 857–884.
- (4) Carmenta, M.; Earnshaw, W. C. The Cellular Geography of Aurora Kinases. *Nat. Rev. Mol. Cell Biol.* **2003**, *4*, 842–854.
- (5) Ducat, D.; Zheng, Y. Aurora Kinases in Spindle Assembly and Chromosome Segregation. *Exp. Cell Res.* **2004**, *301*, 60–67.
- (6) Marumoto, T.; Zhang, D.; Saya, H. Aurora-A, a Guardian of Poles. *Nat. Rev. Cancer* **2005**, *5*, 42–50.
- (7) Barr, A. R.; Gergely, F. Aurora-A: The Maker and Breaker of Spindle Poles. *J. Cell Sci.* **2007**, *120*, 2987–2996.
- (8) Bayliss, R.; Sardon, T.; Vernos, I.; Conti, E. Structural Basis of Aurora-A Activation by TPX2 at the Mitotic Spindle. *Mol. Cell* **2003**, *12*, 851–862.
- (9) Tanaka, T.; Kimura, M.; Matsunaga, K.; Fukada, D.; Mori, H.; Okano, Y. Centrosomal Kinase AIK1 Is Overexpressed in Invasive Ductal Carcinoma of the Breast. *Cancer Res.* **1999**, *59*, 2041–2044.
- (10) Bischoff, J. R.; Anderson, L.; Zhu, Y.; Mossie, K.; Ng, L.; Souza, B.; Schryver, B.; Flanagan, P.; Clairvoyant, F.; Ginther, C.; Chan, C. S. M.; Novotny, M.; Slamon, D. J.; Plowman, G. D. A Homologue of *Drosophila* Aurora Kinase Is Oncogenic and Amplified in Human Colorectal Cancers. *EMBO J.* **1998**, *17*, 3052–3065.
- (11) Gritsko, T. M.; Coppola, D.; Paciga, J. E.; Yang, L.; Sun, M.; Shelley, S. A.; Fiorica, J. V.; Nicosia, S. V.; Cheng, J. Q. Activation and Overexpression of Centrosome Kinase BTAK/Aurora-A in Human Ovarian Cancer. *Clin. Cancer Res.* **2003**, *9*, 1420–1426.
- (12) Reichardt, W.; Jung, V.; Brunner, C.; Klein, A.; Wemmert, S.; Romeike, B. F. M.; Zang, K. D.; Urbschat, S. The Putative Serine/Threonine Kinase Gene *STK15* on Chromosome 20q13.2 Is Amplified in Human Gliomas. *Oncol. Rep.* **2003**, *10*, 1275–1279.
- (13) Chieffi, P.; Troncone, G.; Caleo, A.; Libertini, S.; Linardopoulos, S.; Tramontano, D.; Portella, G. Aurora B Expression in Normal Testis and Seminomas. *J. Endocrinol.* **2004**, *181*, 263–270.
- (14) Araki, K.; Nozaki, K.; Ueba, T.; Tatsuka, M.; Hashimoto, N. High Expression of Aurora-B/Aurora and Ipl1-like Midbody-Associated Protein (AIM-1) in Astrocytomas. *J. Neurooncol.* **2004**, *67*, 53–64.
- (15) Sorrentino, R.; Libertini, S.; Pallante, P. L.; Troncone, G.; Palombini, L.; Bavetsias, V.; Cernia, D. S.; Laccetti, P.; Linardopoulos, S.; Chieffi, P.; Fusco, A.; Portella, G. Aurora B Overexpression Associates with the Thyroid Carcinoma Undifferentiated Phenotype and Is Required for Thyroid Carcinoma Cell Proliferation. *J. Clin. Endocrinol. Metab.* **2005**, *90*, 928–935.
- (16) Mortlock, A. A.; Foote, K. M.; Heron, N. M.; Jung, F. H.; Pasquet, G.; Lohmann, J.-J. M.; Warin, N.; Renaud, F.; De Savi, C.; Roberts, N. J.; Johnson, T.; Dousson, C. B.; Hill, G. B.; Perkins, D.; Hatter, G.; Wilkinson, R. W.; Wedge, S. R.; Heaton, S. P.; Odedra, R.; Keen, N. J.; Crafter, C.; Brown, E.; Thompson, K.; Brightwell, S.; Khatri, L.; Brady, M. C.; Kearney, S.; McKillop, D.; Rhead, S.; Parry, T.; Green, S. Discovery, Synthesis, and in Vivo Activity of a New Class of Pyrazoloquinazolines as Selective Inhibitors of Aurora B Kinase. *J. Med. Chem.* **2007**, *50*, 2213–2224.
- (17) Manfredi, M. G.; Ecsedy, J. A.; Meetze, K. A.; Balani, S. K.; Burenkova, O.; Chen, W.; Galvin, K. M.; Hoar, K. M.; Huck, J. J.; LeRoy, P. J.; Ray, E. T.; Sells, T. B.; Stringer, B.; Stroud, S. G.; Vos, T. J.; Weatherhead, G. S.; Wysong, D. R.; Zhang, M.; Bolen, J. B.; Claiborne, C. F. Antitumour Activity of MLN8054, an Orally Active Small-Molecule Inhibitor of Aurora A kinase. *Proc. Natl. Acad. Sci. U.S.A.* **2007**, *104*, 4106–4111.

- (18) Aliagas-Martin, I.; Burdick, D.; Corson, L.; Dotson, J.; Drummond, J.; Fields, C.; Huang, O. W.; Hunsaker, T.; Kleinheinz, T.; Krueger, E.; Liang, J.; Moffat, J.; Phillips, G.; Pulk, R.; Rawson, T. E.; Ultsch, M.; Walker, L.; Wiesmann, C.; Zhang, B.; Zhu, B.-Y.; Cochran, A. G. A Class of 2,4-Bisanilinopyrimidine Aurora A Inhibitors with Unusually High Selectivity against Aurora B. *J. Med. Chem.* **2009**, *52*, 3300–3307.
- (19) Bouloc, N.; Large, J. M.; Kosmopoulou, M.; Sun, C.; Faisal, A.; Matteucci, M.; Reynisson, J.; Brown, N.; Atrash, B.; Blagg, J.; McDonald, E.; Linardopoulos, S.; Bayliss, R.; Bavetsias, V. Structure-Based Design of Imidazo[1,2-*a*]pyrazine Derivatives as Selective Inhibitors of Aurora-A Kinase in Cells. *Bioorg. Med. Chem. Lett.* **2010**, *20*, 5988–5993.
- (20) Coumar, M. S.; Leou, J.-S.; Shukla, P.; Wu, J.-S.; Dixit, A. K.; Lin, W.-H.; Chang, C.-Y.; Lien, T.-W.; Tan, U.-K.; Chen, C.-H.; Hsu, J. T.-A.; Chao, Y.-S.; Wu, S.-Y.; Hsieh, H.-P. Structure-Based Drug Design of Novel Aurora Kinase A Inhibitors: Structural Basis for Potency and Specificity. *J. Med. Chem.* **2009**, *52*, 1050–1062.
- (21) Prime, M. E.; Courtney, S. M.; Brookfield, F. A.; Marston, R. W.; Walker, V.; Warne, J.; Boyd, A. E.; Kairies, N. A.; von der Saal, W.; Limberg, A.; Georges, G.; Engh, R. A.; Goller, B.; Rueger, P.; Rueth, M. Phthalazinone Pyrazoles as Potent, Selective, and Orally Bioavailable Inhibitors of Aurora-A Kinase. *J. Med. Chem.* **2011**, *54*, 312–319.
- (22) Girdler, F.; Gascoigne, K. E.; Eysers, P. A.; Hartmuth, S.; Crafter, C.; Foote, K. M.; Keen, N. J.; Taylor, S. S. Validating Aurora B as an Anti-Cancer Drug Target. *J. Cell Sci.* **2006**, *119*, 3664–3675.
- (23) Kelly, K. R.; Ecsedy, J.; Mahalingam, D.; Nawrocki, S. T.; Padmanabhan, S.; Giles, F. J.; Carew, J. S. Targeting Aurora Kinases in Cancer Treatment. *Curr. Drug Targets* **2011**, *12*, 2067–2078.
- (24) Malumbres, M. Physiological Relevance of Cell Cycle Kinases. *Physiol. Rev.* **2011**, *91*, 973–1007.
- (25) Otto, T.; Horn, S.; Brockmann, M.; Eilers, U.; Schuttrumpf, L.; Popov, N.; Kenney, A. M.; Schulte, J. H.; Beijersbergen, R.; Christiansen, H.; Berwanger, B.; Eilers, M. Stabilization of N-Myc Is a Critical Function of Aurora A in Human Neuroblastoma. *Cancer Cell* **2009**, *15*, 67–78.
- (26) Brockmann, M.; Poon, E.; Berry, T.; Carstensen, A.; Deubzer, H. E.; Rycak, L.; Jamin, Y.; Thway, K.; Robinson, S. P.; Roels, F.; Witt, O.; Fischer, M.; Chesler, L.; Eilers, M. Small Molecule Inhibitors of Aurora-A Induce Proteasomal Degradation of N-Myc in Childhood Neuroblastoma. *Cancer Cell* **2013**, *24*, 1–15.
- (27) Bavetsias, V.; Large, J. M.; Sun, C.; Bouloc, N.; Kosmopoulou, M.; Matteucci, M.; Wilsher, N. E.; Martins, V.; Reynisson, J.; Atrash, B.; Faisal, A.; Urban, F.; Valenti, M.; de Haven Brandon, A.; Box, G.; Raynaud, F. I.; Workman, P.; Eccles, S. A.; Bayliss, R.; Blagg, J.; Linardopoulos, S.; McDonald, E. Imidazo[4,5-*b*]pyridine Derivatives as Inhibitors of Aurora Kinases: Lead Optimization Studies toward the Identification of an Orally Bioavailable Preclinical Development Candidate. *J. Med. Chem.* **2010**, *53*, 5213–5228.
- (28) Bavetsias, V.; Crumpler, S.; Sun, C.; Avery, S.; Atrash, B.; Faisal, A.; Moore, A. S.; Kosmopoulou, M.; Brown, N.; Sheldrake, P. W.; Bush, K.; Henley, A.; Box, G.; Valenti, M.; de Haven Brandon, A.; Raynaud, F. I.; Workman, P.; Eccles, S. A.; Bayliss, R.; Linardopoulos, S.; Blagg, J. Optimization of Imidazo[4,5-*b*]pyridine-Based Kinase Inhibitors: Identification of a Dual FLT3/Aurora Kinase Inhibitor as an Orally Bioavailable Preclinical Development Candidate for the Treatment of Acute Myeloid Leukemia. *J. Med. Chem.* **2012**, *55*, 8721–8734.
- (29) Larock, R. C.; Yum, E. K. Synthesis of Indoles via Palladium-Catalyzed Heteroannulation of Internal Alkynes. *J. Am. Chem. Soc.* **1991**, *113*, 6689–6690.
- (30) Ujjainwalla, F.; Warner, D. Synthesis of 5-, 6-, and 7-Azaindoles via Palladium-Catalyzed Heteroannulation of Internal Alkynes. *Tetrahedron Lett.* **1998**, *39*, 5355–5358.
- (31) Aadal Nielsen, P.; Brimert, T.; Kristoffersson, A.; Linnanen, T.; Sjo, P. Substituted Pyrrolopyridines. WO2004016609 A1, 2004.
- (32) Finaru, A.; Berthault, A.; Besson, T.; Guillaumet, G.; Berteina-Raboin, S. Microwave-Assisted Solid-Phase Synthesis of 5-Carbox-amido-*N*-acetyltryptamine Derivatives. *Org. Lett.* **2002**, *4*, 2613–2615.
- (33) Yang, D.; Fokas, D.; Li, J.; Yu, L.; Baldino, C. M. A Versatile Method for the Synthesis of Benzimidazoles from *o*-Nitroanilines and Aldehydes in One Step via a Reductive Cyclization. *Synthesis* **2005**, 47–56.
- (34) Davidson, A. H.; Davies, S. J.; Moffat, D. F. C. Quinoline and Quinoxaline Derivatives as Inhibitors of Kinase Enzymatic Activity. WO2006117552 A1, 2006.
- (35) Bolanos-Garcia, V. M. Aurora Kinases. *Int. J. Biochem. Cell Biol.* **2005**, *37*, 1572–1577.
- (36) Dodson, C. A.; Kosmopoulou, M.; Richards, M. W.; Atrash, B.; Bavetsias, V.; Blagg, J.; Bayliss, R. Crystal Structure of an Aurora-A Mutant That Mimics Aurora-B Bound to MLN8054: Insights into Selectivity and Drug Design. *Biochem. J.* **2010**, *427*, 19–28.
- (37) Graczyk, P. P. Gini Coefficient: A New Way To Express Selectivity of Kinase Inhibitors against a Family of Kinases. *J. Med. Chem.* **2007**, *50*, 5773–5779.
- (38) Invitrogen's SelectScreen Profiling. www.invitrogen.com/drugdiscovery (accessed July 22, 2013).
- (39) Bavetsias, V.; Sun, C.; Bouloc, N.; Reynisson, J.; Workman, P.; Linardopoulos, S.; McDonald, E. Hit Generation and Exploration: Imidazo[4,5-*b*]pyridine Derivatives as Inhibitors of Aurora Kinases. *Bioorg. Med. Chem. Lett.* **2007**, *17*, 6567–6571.
- (40) Blagg, J. Structure-Activity Relationships for *in Vitro* and *in Vivo* Toxicity. *Annu. Rep. Med. Chem.* **2006**, *41*, 353–369.
- (41) Kalgutkar, A. S.; Dalvie, D. K.; O'Donnell, J. P.; Taylor, T. J.; Sahakian, D. C. On the Diversity of Oxidative Bioactivation Reactions on Nitrogen-Containing Xenobiotics. *Curr. Drug Metab.* **2002**, *3*, 379–424.
- (42) Shimomura, T.; Hasako, S.; Nakatsuru, Y.; Mita, T.; Ichikawa, K.; Kodaera, T.; Sakai, T.; Nambu, T.; Miyamoto, M.; Takahashi, I.; Miki, S.; Kawanishi, N.; Ohkubo, M.; Kotani, H.; Iwasawa, Y. MK-S108, a Highly Selective Aurora-A Kinase Inhibitor, Shows Antitumour Activity Alone and in Combination with Docetaxel. *Mol. Cancer Ther.* **2010**, *9*, 157–166.
- (43) Manfredi, M. G.; Ecsedy, J. A.; Chakravarty, A.; Silverman, L.; Zhang, M.; Hoar, K. M.; Stroud, S. G.; Chen, W.; Shinde, V.; Huck, J. J.; Wysong, D. R.; Janowick, D. A.; Hyer, M. L.; LeRoy, P. J.; Gershman, R. E.; Silva, M. D.; Germanos, M. S.; Bolen, J. B.; Claiborne, C. F.; Sells, T. B. Characterization of Alisertib (MLN8237), an Investigational Small-Molecule Inhibitor of Aurora A Kinase Using Novel *In Vivo* Pharmacodynamic Assays. *Clin. Cancer Res.* **2011**, *17*, 7614–7624.
- (44) Workman, P.; Collins, I. Probing the Probes: Fitness Factors for Small Molecule Tools. *Chem. Biol.* **2010**, *17*, 561–577.
- (45) Knapp, S.; Arruda, P.; Blagg, J.; Burley, S.; Drewry, D. H.; Edwards, A.; Fabbro, D.; Gillespie, P.; Gray, N. S.; Kuster, B.; Lackey, K. E.; Mazzafera, P.; Tomkinson, N. C. O.; Willson, T. M.; Workman, P.; Zuercher, W. J. A Public-Private Partnership To Unlock the Untargeted Kinome. *Nat. Chem. Biol.* **2013**, *9*, 3–7.
- (46) Dodson, C. A.; Bayliss, R. Activation of Aurora-A Kinase by Protein Partner Binding (TPX2) and Phosphorylation Are Independent and Synergistic. *J. Biol. Chem.* **2012**, *287*, 1150–1157.
- (47) Chan, F.; Sun, C.; Perumal, M.; Nguyen, Q.-D.; Bavetsias, V.; McDonald, E.; Martins, V.; Wilsher, N.; Valenti, M.; Eccles, S.; te Poele, R.; Workman, P.; Aboagye, E. O.; Linardopoulos, S. Mechanism of Action and *In Vivo* Quantification of Biological Activity of the Aurora Kinase Inhibitor CCT129202. *Mol. Cancer Ther.* **2007**, *6*, 3147–3157.
- (48) *Molecular Operating Environment (MOE)*, version 2012.10; Chemical Computing Group Inc.: Montreal, Quebec, Canada, 2011.
- (49) Jones, G.; Willett, P.; Glen, R. C.; Leach, A. R.; Taylor, R. Development and Validation of a Genetic Algorithm for Flexible Docking. *J. Mol. Biol.* **1997**, *267*, 727–748.
- (50) CCP4. The CCP4 (Collaborative Computational Project Number 4) Suite: Programmes for Protein Crystallography. *Acta Crystallogr., D: Biol. Crystallogr.* **1994**, *50*, 760–763.
- (51) Adams, P. D.; Grosse-Kunstleve, R. W.; Hung, L. W.; Ioerger, T. R.; McCoy, A. J.; Moriarty, N. W.; Read, R. J.; Sacchettini, J. C.; Sauter, N. K.; Terwilliger, T. C. PHENIX: Building New Software for Automated Crystallographic Structure Determination. *Acta Crystallogr., D: Biol. Crystallogr.* **2002**, *58*, 1948–1954.